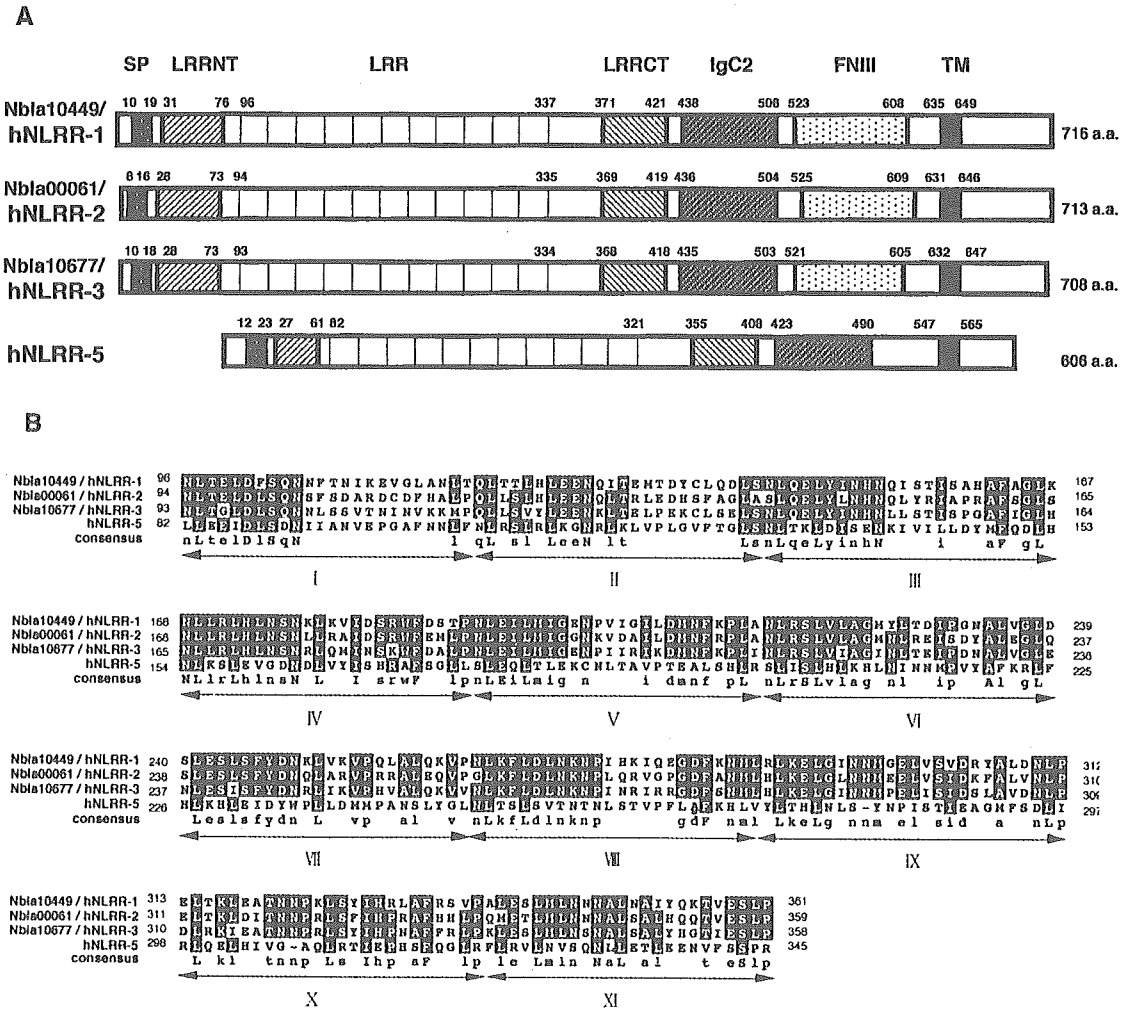

Figure 1. Structures and deduced amino acid sequences of hNLRR families. A, Schematic representation of hNLRR-1, hNLRR-2, hNLRR-3 and hNLRR-5 whose proteins consist of 716, 713, 708 and 606 a.a., respectively. SP, predicted signal peptide; TM, predicted transmembrane region; LRRNT, leucine-rich repeat N-terminal domain; LRRCT, leucine-rich repeat C-terminal domain; LRR, leucine-rich repeat; Igc2, immunoglobulin C-2 type domain; FN III, fibronectin type III domain. B, Amino acid alignment of the LRR domains of hNLRR families. Eleven repeats of LRR motif are shown by Roman numerals. Consensus sequences are highlighted and shown below.

abs. 4P-500 and 4P-501, 2001). h*NLRR-5* has no EGF-like motif and has 11 LRRs, and we failed to identify its human counterpart in the database or our NBL cDNA libraries.

h*NLRR-5*. Homology search against proteins deduced from genomic sequences on chromosome 9p revealed the presence of another family member of NLRR (acc. no. CAC22713). Its deduced protein was 606 a.a. in length and had a similar structure to the other NLRR members. However, a fibronectin domain was not included in this product. It showed 56 and 53% identities to mouse hypothetical protein (acc. no. BAB32403) and *Macaca fascicularis* hypothetical protein (acc. no. BAB03557), respectively, suggesting that they were mouse and *Macaca fascicularis* counterparts of hNLRR-5.

Expression of hNLRR family genes in human tissues. To examine whether *hNLRR* genes display neuron-specific expression, Northern analysis and semi-quantitative RT-PCR were performed. Among several human fetal tissues, h*NLRR-1*, h*NLRR-2* and h*NLRR-3* mRNAs were strongly expressed in brain at the size of 4.0-4.5 kb (Fig. 2A). By contrast, h*NLRR-5* was ubiquitously expressed in all main fetal organs. The size of h*NLRR-2* transcript in the liver was smaller than that in the other tissues. In adult human tissues, all h*NLRR-1*, h*NLRR-2*, h*NLRR-3* and h*NLRR-5* were also preferentially expressed at high levels in the nerve tissues (Fig. 2B).

Expression of hNLRR family genes in neuroblastoma and cell lines. Expression of h*NLRR* family genes was measured in primary neuroblastomas and cell lines using semi-quantitative RT-PCR. As shown in Fig 3A, *Nbla10449/hNLRR-1* was highly expressed in UF NBLs, whereas *Nbla10677/hNLRR-3* and h*NLRR-5* were preferentially expressed in the F NBLs. *Nbla00061/hNLRR-2* seemed to be equally expressed between both subsets. In NBL cell lines, expression of *NLRR-1* was observed relatively more frequently in the lines with *MYCN* amplification than in those with a single copy of the gene. On the other hand, *NLRR-3* appeared to be expressed rather frequently in the cell lines without *MYCN* amplification. Interestingly, however, there was a tendency that the cells with high expression of *NLRR-1* also had a high levels of expression of *NLRR-3* (Fig. 3B). The expression of both h*NLRR-2* and h*NLRR-5* was found in most NBL cell lines.

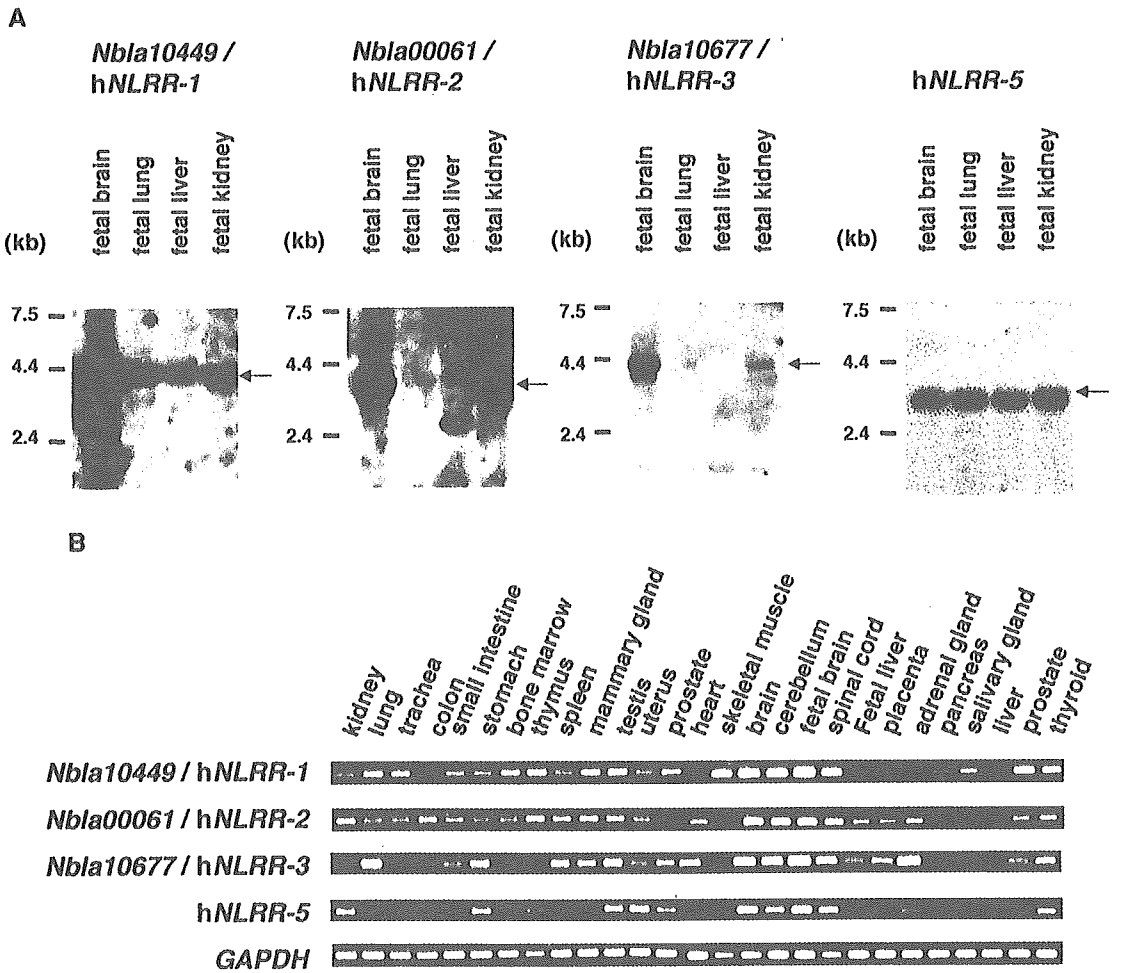

Figure 2. Expression of h*NLRR*s mRNA in human normal tissues. A, Northern blot analysis of h*NLRR*s mRNA in human fetal tissues. As a control for the amount of RNA, the same filter was rehybridized with ß-actin. B, Semi-quantitative RT-PCR of h*NLRR*s in multiple human tissues. Total RNA of 25 adult and 2 fetal tissues. As a control, same cDNA templates were amplified by *GAPDH* primers.

We then examined whether or not there was any genomic amplification of h*NLRR-1* or h*NLRR-2* because that of *Nbla10449/hNLRR-1* was preferentially expressed in UF NBLs, and that of *GAC1/hNLRR-2* was reported to be amplified in the primary glioblastoma and anaplastic astrocytoma (15). However, our Southern blot analysis showed that neither of both genes was amplified in NBL cell lines so far examined (CHP134, IMR32, NB-9, NLF, TGW, NGP, NB69, NBL-S, SK-N-AS and SH-SY5Y) (data not shown). As regards the other cancer cell lines, expression of h*NLRR* family members was relatively restricted to the osteosarcoma and rhabdomyosarcoma cell lines (Fig. 3C). The low levels of h*NLRR*-3 and h*NLRR-5* expression were also seen in melanoma cell lines. Furthermore, expression of h*NLRR-2* was observed in the cell lines of colon, thyroid (medullary thyroid cancer), esophagus and lung. These results suggested that h*NLRR*s were preferentially expressed in the cell lines derived from neural crest cells.

Changes in expression of the NLRR family genes during NGF-induced differentiation and NGF-depletion-induced apoptosis in newborn mouse SCG neurons in primary culture. To investigate the role of NLRR family molecules in NGF/TrkA-mediated signaling, we next used newborn mouse SCG neurons, from which NBL is derived. As reported previously, NGF induced marked morphological differentiation of SCG neurons (14). NGF-induced neurite extension was observed on day 2 and was enhanced thereafter by increasing in number and length (Fig. 4A, NGF^+). The depletion of NGF by treating the cells with anti-NGF antibody induced neuronal programmed cell death (Fig. 4A, NGF^-). As shown in Fig. 4B, expression of m*NLRR-1* and m*NLRR-5* was down-regulated during NGF-induced neuronal differentiation, and was up-regulated after NGF deprivation (Fig. 4B). On the other hand, expression of m*NLRR-2* and m*NLRR-3* was slightly up-regulated when they were treated with NGF, and was significantly down-regulated after NGF deprivation (Fig. 4B), suggesting that expression of m*NLRR* genes might be related to the NGF signaling.

Prognostic significance of expression of Nbla10449/hNLRR-1 and Nbla10677/hNLRR-3 in primary neuroblastomas. To evaluate the clinical significance, expression of *Nbla10449/* h*NLRR-1* and *Nbla10677/*h*NLRR-3* in 99 NBLs was statistically analyzed. Table I gives the mean and standard error (SEM) of h*NLRR-1/Nbla10449* and h*NLRR-3/Nbla10677*

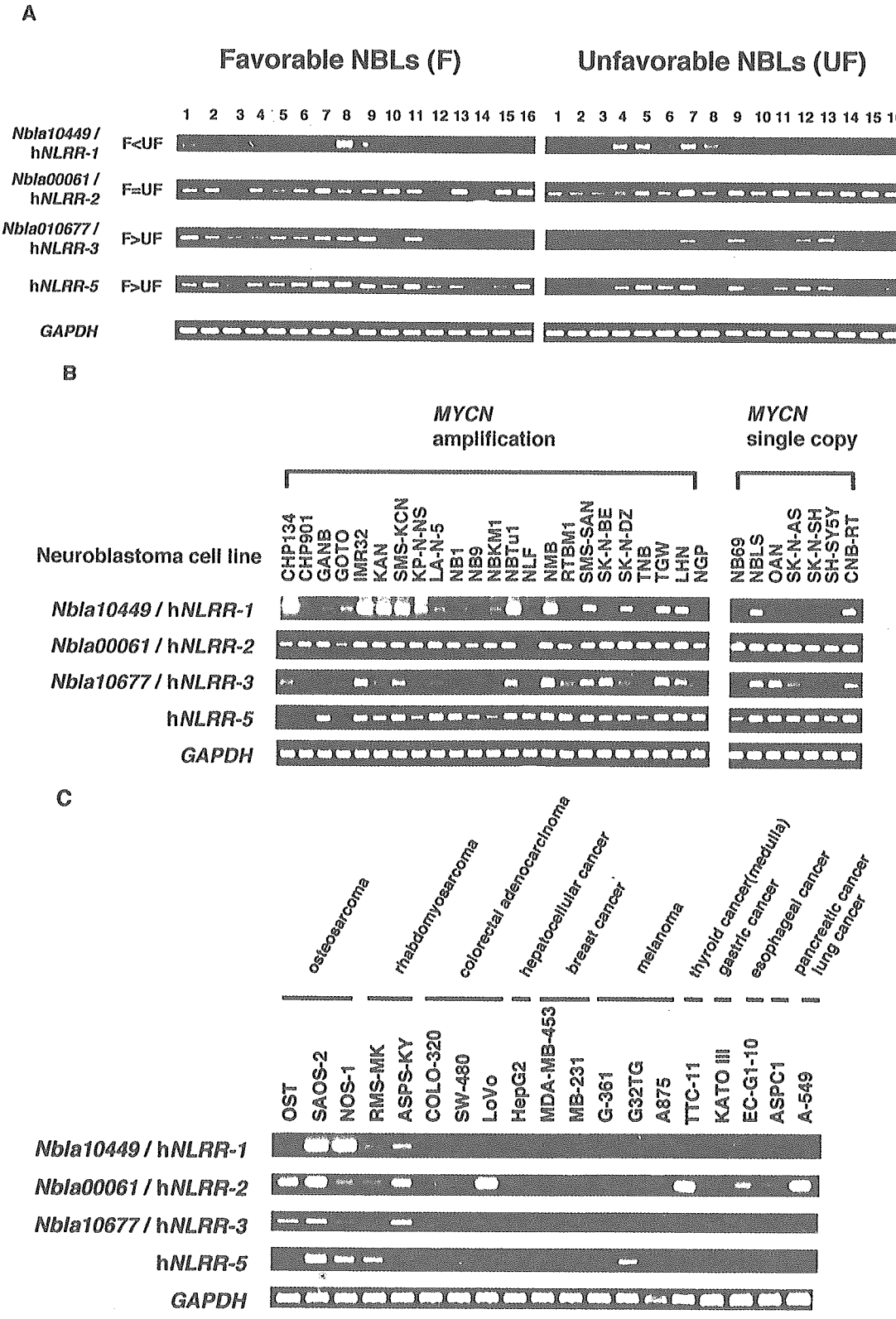

Figure 3. Expression of h*NLRR* family genes in primary NBLs, NBL cell lines and other cancer cell lines. A, Differential expression of h*NLRR* family genes in 16 favorable and 16 unfavorable NBLs. mRNA expression was detected by semi-quantitative RT-PCR procedure. The expression of *GAPDH* is shown as a control. Lanes 1-16: favorable NBLs (F, stage 1 or 2, with a single copy of *MYCN*), lanes 17-32: unfavorable NBLs (UF, stage 3 or 4, with *MYCN* amplification). B, Expression of h*NLRR*s mRNA in NBL cell lines. Twenty-three NBL cell lines with *MYCN* amplification and 7 cell lines with a single copy of *MYCN* were used for semi-quantitative RT-PCR as templates. C, Expression of h*NLRR*s mRNA in the other cancer cell lines. Semi-quantitative RT-PCR analysis was performed using cDNA and control *GAPDH* primers. Tumor origins are shown on the top.

expression by age, tumor stage, *TrkA* expression, *MYCN* copy number, origin, and mass screening. High expression of h*NLRR-1/Nbla10449* were significantly associated with >1 year of age (p=0.0001), advanced stage (p=0.0007), low expression of *TrkA* (p=0.011), *MYCN* amplification (p=0.0001) and sporadic tumors (p=0.0004), but not with the tumor origin (p=0.4). The results of log-rank test showed that a high level of h*NLRR-1/Nbla10449* expression was significantly associated

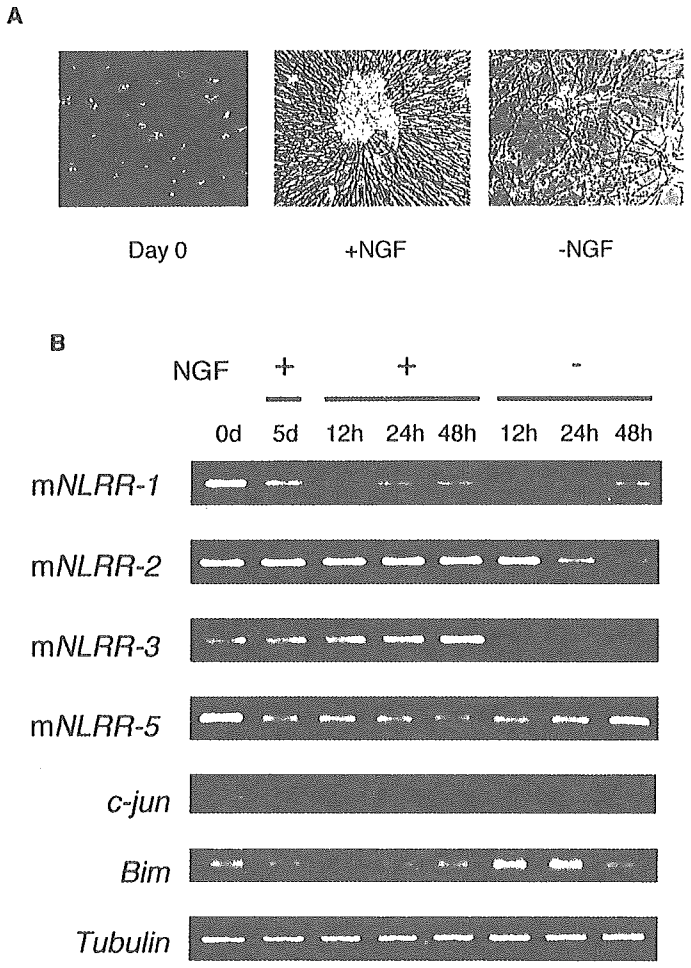

Figure 4. Changes in mRNA expression of mouse *NLRR* family genes in mouse superior cervical ganglion (SCG) cells treated with NGF in primary culture. A, Effect of NGF on newborn mouse SCG neurons in primary culture. The pictures were taken on day 0 and 5 (NGF^+) in the presence of 50 ng/ml NGF. NGF was then depleted from the medium by adding 1% v/v anti-NGF antibody for 36 h (NGF^-). B, Changes in expression of m*NLRR*s mRNA during NGF-induced differentiation and NGF depletion-induced apoptosis in newborn mouse SCG neurons in primary culture. SCG neurons were cultured for 5 days with NGF and then further cultured with or without NGF for 12, 24, 48 h. *c-jun* and *Bim*, positive control gene; Tubulin, used for standardization of the cDNA concentration.

with an unfavorable outcome (p=0.028). On the other hand, there was significant correlation between high levels of *Nbla10677/*h*NLRR-3* expression and younger age (p=0.0018), favorable stage (p=0.0007), high levels of *TrkA* expression (p=0.021), single copy of *MYCN* (p=0.0002) and the tumors found by mass screening (p=0.0049), but not with the tumor origin (p=0.33).

The univariate Cox regression was employed to examine the individual relationship of each variable to survival (Table II). These variables were: h*NLRR-1/Nbla10449* (log), h*NLRR-3/Nbla10677* (log), age (>1 year vs. <1 year), tumor stage (3+4 vs. 1+2+4s, *MYCN* copy number (1 copy vs. >1 copy), mass screening (+ vs. -), and origin (adrenal gland vs. others). Expression of h*NLRR-1/Nbla10449* (p=0.005), age (p<0.0005), *MYCN* copy number (p<0.0005), mass screening (p=0.001) were found to be statistically of prognostic importance. The results in Table II show that h*NLRR-1/*

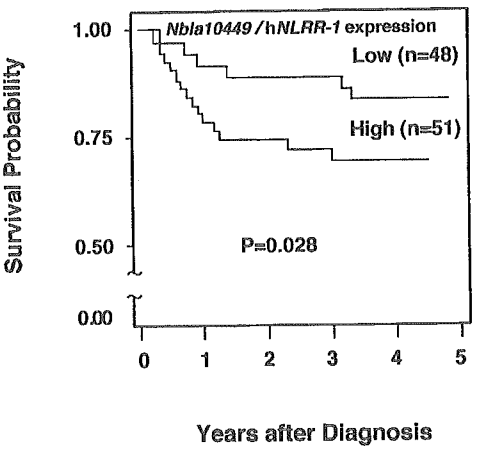

Figure 5. Kaplan-Meier survival curves for the 48 patients with low expression and the 51 patients with high expression.

Nbla10449 expression was an independent prognostic factor from age, *MYCN* copy number and mass screening in primary NBLs.

Discussion

In the present study, we identified the full-length human neuronal leucine-rich repeat protein (*NLRR*) family genes preferentially expressed in the nervous system and adrenal gland: *Nbla10449/*h*NLRR-1*, *Nbla00061/*h*NLRR-2/GAC1*, *Nbla10677/*h*NLRR-3* and h*NLRR-5*. In primary NBLs, the levels of h*NLRR-1* expression are significantly higher in the unfavorable subsets than those in the favorable tumors, whereas the expression pattern of h*NLRR-3* and h*NLRR-5* is the opposite. The results from the experiments using mouse SCG neurons treated with NGF in the primary culture have suggested that both m*NLRR-2* and *NLRR-3* are the molecules relating to promotion of neuronal survival or differentiation, while m*NLRR-1* and m*NLRR-5* function as those promoting cell growth or enhancing apoptosis. Furthermore, expression of h*NLRR-1* has been found as a significant indicator of poor outcome of NBLs, whereas that of h*NLRR-3* is associated with other favorable prognostic factors. Thus, hNLRR family members appear to differently regulate functions of neuronal cells as well as those of neuroblastoma.

A protein with leucine-rich repeat (LRR) domains was first identified in an α-2-glycoprotein of human serum (17). LRR-containing proteins represent a diverse group of molecules with different functions and cellular locations in a variety of organs. LRR domains provide an ideal conformation for binding to other proteins and this structure is thought to be involved in protein-protein interaction (10). Many LRR-containing proteins have been shown to function as cell-adhesion molecules or signaling receptors and are implicated in a variety of events in neural development. For example, adhesive LRR-containing proteins and small proteoglycans such as osteoinductive factor (OIF) bind various components of the extracellular matrix and growth factors. Interestingly, OIF binds the transforming growth factors, TGF-ß and TGF-ß2, and is involved in bone formation (18). The neurotrophin receptors, Trks, also possess the LRR domains in the extra-

Table I. Correlation between expression of *Nbla10449/hNLRR-1* or *Nbla10677/hNLRR-3* and other prognostic factors (Student's t-test).

Variable	No.	*Nbla10449/hNLRR-1*		*Nbla10677/hNLRR-3*	
		Mean ± SEM	p-value	Mean ± SEM	p-value
Age					
<1 year	63	0.84±0.21	0.0001	5.05±0.93	0.0018
>1 year	36	3.97±1.44		2.53±0.77	
Tumor stage					
1, 2, 4s	57	0.68±0.17	0.0007	5.36±1.00	0.0007
3, 4	42	3.74±1.25		2.48±0.68	
TrkA expression					
Low	45	3.50±1.17	0.011	3.13±0.77	0.021
High	54	0.71±0.18		4.97±1.02	
MYCN copy no.					
Amplified	29	5.19±1.75	0.0001	1.71±0.90	0.0002
Single	70	0.65±0.14		5.14±0.86	
Origin					
Adrenal gland	63	2.16±0.75	0.4	4.18±0.90	0.33
Others	36	1.67±0.79		4.06±0.93	
Mass screening					
+	54	0.67±0.18	0.0004	5.09±1.02	0.0049
-	45	3.55±1.17		2.98±0.76	

Table II. Cox regression models using *Nbla10449/hNLRR-1* expression and dichotomous factors of age, *TrkA* expression, *MYCN* amplification, and origin (n=99).

Model	Variable	p-value
A	*Nbla10449/hNLRR-1*	0.005
B	*Nbla10677/hNLRR-3*	0.15
C	Age (>1 vs. <1 year)	<0.005
D	*MYCN* (1 copy vs. amplification)	<0.005
E	Origin (adrenal gland vs. others)	0.079
F	Mass screening (+ vs. -)	0.001

cellular region. In *Drosophila*, some LRR domain-containing molecules such as toll, slit, connectin, chaoptin and tartan play an important role in regulating neural development (19-23).

The LRR motif includes highly hydrophobic amino acids and a repeat structure consisting of about 24 residues (20). NLRR family proteins contain in its extracellular region an immunoglobulin C-2 type domain and a fibronectin type III domain in addition to 11 sets of LRR motif (24). *NLRR* family genes were first isolated from a mouse brain cDNA library (16,25), and then 3 distinct isoforms (m*NLRR-1*, m*NLRR-2* and m*NLRR-3*) have been identified in zebrafish, *Xenopus*, mouse, rat and *Macaca facicularis* (16,24-26). The function of these NLRR proteins is poorly understood except that expression of m*NLRR-3* was increased after cortical brain injury (27) and that *rNLRR-3* expression is regulated through the Ras-MAPK signaling pathway in fibroblasts (28).

The deduced amino acid sequences of hNLRRs are highly conserved in the domains of LRR, LRRNT, LRRCT, Igc2 and FNIII, except that h*NLRR-5* does not have the FNIII domain. Many LRR proteins with LRRNT and LRRCT domains have been proposed to function in the regulation of neural differentiation and/or developmental processes as adhesive proteins and/or receptors (10). In addition to LRR, the Igc2 and FNIII domains in the extracellular region are often found in the molecules expressed in the central nervous system (26) and in several neuronal cell-adhesion molecules of the immunoglobulin superfamily such as N-CAM and L1 (29). Although hNLRRs and other NLRRs have no known signaling domain in the cytoplasmic region, a number of conserved stretches are found (Fig. 1). Especially, NLRR-1 and NLRR-3 have been shown to have a conserved stretch of 11 amino acids (ELYPPLINLWE) with 2 clathrin mediated endocytosis motifs, a tyrosine-based signal conforming to the YXRF motif (30,31), and a dileucine-type motif (32). Endocytosis and recycling mechanisms are relevant for cell adhesion molecules like integrins during cell migration (33,34).

Although the function of NLRR protein is poorly understood, there are some clues in recent reports. mNLRR-3 expression is increased in layers 2-3 in cerebral cortex after cortical injury, suggesting that this molecule plays a role in

the regulation of synaptic re-organization (27). zNLRR has also been proposed to have function as a neuronal-specific adhesion molecule or soluble ligand binding receptor during regeneration of the zebrafish central nervous system after injury, because retinal ganglion cells and descending spinal cord neurons strongly increased expression of z*NLRR* after axotomy in the adult (24).

The SCG/NGF system utilized in this study also provides a helpful hint to consider the neuronal function of hNLRRs. NLRR-1 may be involved in growth promotion in NBL by suppressing neuronal differentiation according to the result showing that the expression of m*NLRR-1* is down-regulated when the cells were treated with NGF. On the other hand, NLRR-3 may play a role in regulating differentiation to extend neurites and in neuronal survival of NBL cells since the expression of m*NLRR-3* was up-regulated by NGF and down-regulated after deprivation of NGF. These results are consistent with their differential expression pattern between favorable and unfavorable subsets of NBL.

In favorable NBLs as well as the cell lines with a single copy of *MYCN*, h*NLRR-1* expression was low as compared with the *MYCN*-amplified cells, suggesting that MYCN could influence the h*NLRR-1* expression. Interestingly, we have identified MYCN transcription factor-binding motifs (E-boxes) in the promoter region of the *NLRR-1* gene. Like h*NLRR-3*, h*NLRR-2* may also be involved in controlling neural cell survival as supposed from the result obtained in the NGF/SCG system. Ubiquitous h*NLRR-2* expression in NBLs suggests that h*NLRR-2* plays a role in maintaining cell survival. Of interest, h*NLRR-2* is often amplified in glioma as described below. h*NLRR-5* shows similar change in expression to h*NLRR-1* in the system of NGF-treated SCG neurons, albeit it is highly expressed in favorable NBLs. This suggests that hNLRR-5 may function as a proapoptotic molecule in NBL. Thus, each hNLRR member may have distinct biological function in NBL as well as neuronal cells. As the deduced intracellular region at the extreme C-terminus of hNLRR proteins has variable amino acid sequences, it may play a role in determining the differential function of hNLRR family receptors.

There are a few reports showing the relationship between LRR or NLRR and human cancer. *GAC1* (*hNLRR-2*), mapped to chromosome 1q32.1, is amplified and overexpressed in glioblastoma multiforme and anaplastic astrocytoma (15). Another report shows that expression of r*NLRR-3*, which was cloned by the subtractive screening using fibrosarcoma cells overexpressing c-Ha-ras, is regulated through the Ras-MAPK pathway, albeit the role in cancer cells is unknown (28). Trk family receptor tyrosine kinases have 3 LRRs in the extracellular domain, whose alteration can cause onco genic activation in some cancers (35). Interestingly, TrkA and TrkB also show an inverse expression pattern between favorable and unfavorable NBLs, that is very similar to the pattern of h*NLRR-1* and h*NLRR-3* expression. Since expression levels of TrkA and TrkB are powerful prognostic factors in NBLs, those of h*NLRR-1* and h*NLRR-3* may also be important in predicting the patient's outcome. Indeed, our present data suggest that expression of both hNLRR-1 and hNLRR-3 is inversely associated with the prognosis as well as other prognostic factors.

Acknowledgements

The authors thank Drs M. Fukumura, and H. Tsunobuchi for helpful discussions, Drs H. Kageyama and K. Miyazaki for experimental support, Dr S. Sakiyama for encouragement, and Ms. N. Sugimitsu and A. Morohashi for their excellent technical assistance. The authors also thank the following institutes for providing surgical samples: First Department of Surgery, Hokkaido University School of Medicine; Department of Pediatrics, National Sapporo Hospital; Department of Pediatric Surgery, Tohoku University School of Medicine; Department of Surgery, Gunma Children's Medical Center; Department of Pediatrics, Pediatric Surgery and General Surgery, Jichi Medical University; Department of Hematology and Oncology, Saitama Children's Medical Center; Department of Pediatrics, Juntendo University School of Medicine; Department of Surgery, Kiyose Metropolitan Children's Hospital; Department of Surgery and Pathology, Chiba Children's Hospital; Department of Pediatric Surgery, Chiba University School of Medicine; Department of Pediatric Surgery, Kimitsu Central Hospital; Department of Pediatric Surgery, Niigata University School of Medicine; Department of Pediatrics and Pediatric Surgery, Aichi Medical University; Department of Pediatrics, Kyoto Prefectural Medical University; Tumor Board, Hyogo Children's Hospital; Department of Pediatrics and Pediatric Surgery, Kagoshima University School of Medicine; Department of Pediatric Surgery, Showa University School of Medicine; Department of Pediatrics, Oita University School of Medicine; Department of Pediatric Surgery, Ohta General Hospital; Department of Pediatrics, Ichinomiya City Hospital; Department of Pediatric Surgery, Osaka City General Hospital; Department of Pediatrics, Nihon University School of Medicine Itabashi Hospital; Department of Pediatric Surgery, University of Tsukuba School of Medicine.

References

1. Bolande RP: The neurocristopathies. A unifying concept of disease arising in neural crest maldevelopement. Hum Pathol 5: 409-429, 1974.
2. Lo L, Morin X, Brunet JF and Anderson DJ: Specification of neurotransmitter identity by Phox2 proteins in neural crest stem cells. Neuron 22: 693-705, 1999.
3. Nakagawara A, Arima-Nakagawara M, Scavarda NJ, Azar CG, Cantor AB and Brodeur GM: Association between high levels of expression of the TRK gene and favorable outcome in human neuroblastoma. N Engl J Med 328: 847-854, 1993.
4. Nakagawara A, Azar CG, Scavarda NJ and Brodeur GM: Expression and function of TRK-B and BDNF in human neuroblastomas. Mol Cell Biol 14: 759-767, 1994.
5. Lasorella A, Noseda M, Beyna M, Yokota Y and Iavarone A: Id2 is a retinoblastoma protein target and mediates signaling by Myc oncoprotein. Nature 407: 592-598, 2000.
6. Ohira M, Shishikura T, Kawamoto T, Inuzuka H, Morohashi A, Takayasu H, Kageyama H, Takada N, Takahashi M, Sakiyama S, Suzuki Y, Sugano S, Kuma H, Nozawa I and Nakagawara A: Hunting the subset-specific genes of neuroblastoma: expression profiling and differential screening of the full-length-enriched oligo-capping cDNA libraries. Med Pediatr Oncol 35: 547-549, 2000.
7. Suzuki Y, Yoshitomo-Nakagawa K, Maruyama K, Suyama A and Sugano S: Construction and characterization of a full length-enriched and a 5'-end-enriched cDNA library. Gene 200: 149-156, 1997.

8. Ohira M, Morohashi A, Inuzuka H, Shishikura T, Kawamoto T, Kageyama T, Nakamura Y, Isogai E, Takayasu H, Sakiyama S, Suzuki Y, Sugano S, Goto T, Sato S and Nakagawara A: Expression profiling and characterization of 4200 genes cloned from primary neuroblastomas: identification of 305 genes differentially expressed between favorable and unfavorable subsets. Oncogene 22: 5525-5536, 2003.
9. Ohira M, Morohashi A, Nakamura Y, Isogai E, Furuya K, Hamano S, Machida T, Aoyama, Fukumura M, Miyazaki K, Suzuki Y, Sugano S, Hirato J and Nakagawara A: Neuroblastoma oligo-capping cDNA project: toward the understanding of the genesis and biology of neuroblastoma. Cancer Lett 197: 63-68, 2003.
10. Kobe B and Deisenhofer J: The leucine-rich repeat: a versatile binding motif. Trends Biochem Sci 19: 415-421, 1994.
11. Shimada H, Chatten J, Newton WA Jr, Sachs N, Hamoudi AB, Chiba T, Marsden HB and Misugi K: Histopathologic prognostic factors in neuroblastic tumors: definition of subtypes of ganglioneuroblastoma and an age-linked classification of neuroblastomas. J Natl Cancer Inst 73: 405-416, 1984.
12. Brodeur GM, Pritchard J, Berthold F, Carlsen NL, Castel V, Castelberry RP, De Bernardi B, Evans AE, Favrot M and Hedborg F: Revisions of the international criteria for neuroblastoma diagnosis, staging and response to treatment. J Clin Oncol 11: 1466-1477, 1993.
13. Kaneko M, Nishihira H, Mugishima H, Ohnuma N, Nakada K, Kawa K, Fukuzawa M, Suita S, Sera Y and Tsuchida Y: Stratification of treatment of stage 4 neuroblastoma patients based on N-myc amplification status. Study Group of Japan for Treatment of Advanced Neuroblastoma, Tokyo, Japan. Med Pediatr Oncol 31: 1-7, 1998.
14. Smith CJ, Johnson EM Jr, Osborne P, Freeman RS and Neveu I and Brachet P: NGF deprivation and neuronal degeneration trigger altered beta-amyloid precursor protein gene expression in the rat superior cervical ganglia *in vivo* and *in vitro*. Brain Res Mol Brain Res 17: 328-334, 1993.
15. Almeida A, Zhu XX, Vogt N, Tyagi R, Muleris M, Dutrillaux AM, Dutrillaux B, Ross D, Malfoy B and Hanash S: GAC1, a new member of the leucine-rich repeat superfamily on chromosome band 1q32.1, is amplified and overexpressed in malignant gliomas. Oncogene 16: 2997-3002, 1998.
16. Taguchi A, Wanaka A, Mori T, Matsumoto K, Imai Y, Tagaki T and Tohyama M: Molecular cloning of novel leucine-rich repeat proteins and their expression in the developing mouse nervous system. Brain Res Mol Brain Res 35: 31-40, 1996.
17. Takahashi N, Takahashi Y and Putnam FW: Periodicity of leucine and tandem repetition of a 24-amino acid segment in the primary structure of leucine-rich alpha 2-glycoprotein of human serum. Proc Natl Acad Sci USA 82: 1906-1910, 1985.
18. Kresse H, Hausser H and Schonherr E: Small proteoglycans. Experientia 49: 403-416, 1993.
19. Lemaitre B, Nicolas E, Michaut L, Reichhart JM and Hoffmann JA: The dorsoventral regulatory gene cassette spatzle/Toll/cactus controls the potent antifungal response in *Drosophila* adults. Cell 86: 973-983, 1996.
20. Rothberg JM, Jacobs JR, Goodman CS and Artavanis-Tsakonas S: Slit: an extracellular protein necessary for development of midline glia and commissural axon pathways contains both EGF and LRR domains. Genes Dev 4: 2169-2187, 1990.
21. Nose A, Mahajan VB and Goodman CS: Connectin: a homophilic cell adhesion molecule expressed on a subset of muscles and the motoneurons that innervate them in *Drosophila*. Cell 70: 553-567, 1992.
22. Krantz DE and Zipursky SL: *Drosophila chaoptin*, a member of the leucine-rich repeat family, is a photoreceptor cell-specific adhesion molecule. EMBO J 9: 1969-1977, 1990.
23. Chang Z, Price BD, Bockheim S, Boedigheimer MJ, Smith R and Laughon A: Molecular and genetic characterization of the *Drosophila tartan* gene. Dev Biol 160: 315-332, 1993.
24. Bormann P, Roth LW, Andel D, Ackermann M and Reinhard E: zfNLRR, a novel leucine-rich repeat protein is preferentially expressed during regeneration in zebrafish. Mol Cell Neurosci 13: 167-179, 1999.
25. Taniguchi H, Tohyama M and Takagi T: Cloning and expression of a novel gene for a protein with leucine-rich repeats in the developing mouse nervous system. Brain Res Mol Brain Res 36: 45-52, 1996.
26. Hayata T, Uochi T and Asashima M: Molecular cloning of XNLRR-1, a *Xenopus* homolog of mouse neuronal leucine-rich repeat protein expressed in the developing *Xenopus* nervous system. Gene 221: 159-166, 1998.
27. Ishii N, Wanaka A and Tohyama M: Increased expression of NLRR-3 mRNA after cortical brain injury in mouse. Brain Res Mol Brain Res 40: 148-152, 1996.
28. Fukamachi K, Matsuoka Y, Kitanaka C, Kuchino Y and Tsuda H: Rat neuronal leucine-rich repeat protein-3: cloning and regulation of the gene expression. Biochem Biophys Res Commun 287: 257-263, 2001.
29. Brummendorf T and Rathjen FG: Structure/function relationships of axon-associated adhesion receptors of the immunoglobulin superfamily. Curr Opin Neurobiol 6: 584-593, 1996.
30. Chen WJ, Goldstein JL and Brown MS: NPXY, a sequence often found in cytoplasmic tails, is required for coated pit-mediated internalization of the low density lipoprotein receptor. J Biol Chem 265: 3116-3123, 1990.
31. Collawn JF, Stangel M, Kuhn LA, Esekogwu V, Jing SQ, Trowbridge IS and Tainer JA: Transferrin receptor internalization sequence YXRF implicates a tight turn as the structural recognition motif for endocytosis. Cell 63: 1061-1072, 1990.
32. Kirchhausen T: Clathrin. Annu Rev Biochem 69: 699-727, 2000.
33. Lauffenburger DA and Horwitz AF: Cell migration: a physically integrated molecular process. Cell 84: 359-369, 1996.
34. Lawson MA and Maxfield FR: Ca(2+)- and calcineurin-dependent recycling of an integrin to the front of migrating neutrophils. Nature 377: 75-79, 1995.
35. Meakin SO and Shooter EM: The nerve growth factor family of receptors. Trends Neurosci 15: 323-231, 1992.

THE JOURNAL OF BIOLOGICAL CHEMISTRY
Vol. 279, No. 24, Issue of June 11, pp. 25549–25561, 2004
Printed in U.S.A.

Polo-like Kinase 1 (Plk1) Inhibits p53 Function by Physical Interaction and Phosphorylation*

Received for publication, December 26, 2003, and in revised form, March 11, 2004
Published, JBC Papers in Press, March 15, 2004, DOI 10.1074/jbc.M314182200

Kiyohiro Ando‡§¶, Toshinori Ozaki‡¶, Hideki Yamamoto‡, Kazushige Furuya‡, Mitsuchika Hosoda‡, Syunji Hayashi‡, Masahiro Fukuzawa§, and Akira Nakagawara‡‖

From the ‡Division of Biochemistry, Chiba Cancer Center Research Institute, Chiba 260-8717, Japan and the §First Department of Surgery, Nihon University School of Medicine, Tokyo 173-8610, Japan

Polo-like kinase 1 (Plk1) has an important role in the regulation of M phase of the cell cycle. In addition to its cell cycle-regulatory function, Plk1 has a potential role in tumorigenesis. Here we found for the first time that Plk1 physically binds to the tumor suppressor p53 in mammalian cultured cells, and inhibits its transactivation activity as well as its pro-apoptotic function. During the cisplatin-induced apoptosis in human neuroblastoma SH-SY5Y cells, the expression level of Plk1 was significantly decreased both at mRNA and protein levels, whereas cisplatin treatment caused a remarkable stabilization of p53. Systematic immunoprecipitation analyses using a series of deletion mutants of p53 revealed that a sequence-specific DNA-binding region of p53 is required and sufficient for the physical interaction with Plk1. The ectopically overexpressed Plk1 was co-localized with the endogenous p53 in mammalian cell nucleus, as shown by confocal laser microscopy. Expression of exogenous Plk1 and p53 in p53-deficient lung carcinoma H1299 cells greatly decreased the p53-mediated transcription from the p53-responsive *p21*^{WAF1}, *MDM2*, and *BAX* promoters, whereas the kinase-deficient mutant form of Plk1 failed to reduce the transcriptional activity of p53. Consistent with the luciferase reporter analysis, Plk1 had an ability to block the p53-dependent induction of the endogenous p21^{WAF1}. In addition, Plk1 inhibited the pro-apoptotic function of p53 in H1299 cells. Intriguingly, Plk1-mediated repression of p53 was attenuated with ATM. Thus, our present findings strongly suggest that p53 is a critical target of Plk1, and its function is abrogated through the physical interaction with Plk1.

The polo-like kinases (Plks)[1] are structurally and functionally related to the *Drosophila* polo serine/threonine (Ser/Thr) kinase (1), and are evolutionarily well conserved from yeast to mammals. A high degree of amino acid sequence similarity is detected within a catalytic domain and a unique noncatalytic domain (termed the polo-box) located at the NH_2- and COOH-terminal region, respectively (2). It has been shown that the polo-box is critical for the correct subcellular localization of Plks (3, 4), and the COOH-terminal region containing the polo-box serves to regulate its kinase activity (5). A growing body of evidence obtained in various experimental systems suggests that Plks play an important role in the regulation of a variety of M-phase-specific events including entry into and exit from mitosis (1, 6–8). In addition to their critical role during the G_2/M transition, Plks might be also required for G_1/S phase transition (9, 10).

In mammalian cells, there exist at least three Plk family members including Plk1, Plk2, and Plk3. Plk1 (also referred to as Plk) has been identified as a serine/threonine kinase that displays an extensive amino acid sequence homology to *Drosophila* polo (2, 9, 11–13), whereas Plk2 (alternatively named Snk) and Plk3 (alternatively termed as proliferation related kinase, Prk) have been originally shown to be transcriptionally induced in response to mitogens (14, 15). In mammalian cultured cells, the amounts of Plk1 mRNA and protein are regulated in a cell cycle-dependent manner, rising from a very low level in G_1 phase to a maximal level during G_2/M phase (11, 12). The kinase activity of Plk1 is regulated by its phosphorylation and peaks at M phase (16–18). Recently, it has been shown that the kinase activity of Plk1 is inhibited in response to DNA damage in mammalian cultured cells and this inhibition occurs in an ATM-dependent manner (19, 20). Plk1 phosphorylates various substrate proteins including cyclin B1 and Cdc25C. At the onset of mitosis, Plk1 phosphorylated cyclin B1 and promoted rapid nuclear translocation of an active Cdc2-cyclin B1 complex (21, 22). In addition, Toyoshima-Morimoto *et al.* (23) has found that, during G_2/M phase, Plk1 is capable of phosphorylating Cdc25C, which dephosphorylates and directly activates the Cdc2-cyclin B1 complex, and regulating the nuclear entry of Cdc25C. In contrast to Plk1, the expression level of Plk3 remains constant during the cell cycle progression and its kinase activity peaks during late S and G_2 phase (24, 25). Xie *et al.* (26) found that the kinase activity of Plk3 is rapidly increased in response to DNA damage in an ATM-dependent fashion.

In addition to the potential cell cycle-regulatory role, Plk1 has been implicated in the genesis and/or progression of tumors. *Plk1* was overexpressed in rapidly proliferating cells as well as various human primary tumors (27), suggesting that the expression level of *Plk1* is tightly linked to proliferation and could be used as a negative prognostic indicator for various

* This work was supported in part by a grant-in-aid from the Ministry of Health and Welfare for a New 10-Year Strategy for Cancer Control, a grant-in-aid for Scientific Research on Priority Areas, a grant-in-aid for Scientific Research (B) from the Ministry of Education, Science, Sports and Culture, Japan, and the Hisamitsu Pharmaceutical Company. The costs of publication of this article were defrayed in part by the payment of page charges. This article must therefore be hereby marked "*advertisement*" in accordance with 18 U.S.C. Section 1734 solely to indicate this fact.

¶ Both authors contributed equally to this work.

‖ To whom correspondence should be addressed: Division of Biochemistry, Chiba Cancer Center Research Institute, 666-2 Nitona, Chuoh-ku, Chiba 260-8717, Japan. Tel.: 81-43-264-5431; Fax: 81-43-265-4459; E-mail: akiranak@chiba-ccri.chuo.chiba.jp.

[1] The abbreviations used are: Plk, polo-like kinase; ATM, ataxia telangiectasia mutated; GFP, green fluorescence protein; GST, glutathione *S*-transferase; NLS, nuclear localization signal; NMS, normal mouse serum; PBS, phosphate-buffered saline; TBS, Tris-buffered saline; TK, thymidine kinase; RT, reverse transcriptase.

tumors (28–30). Consistent with these observations, constitutive overexpression of Plk1 in NIH3T3 cells resulted in the oncogenic focus formation and induction of tumor growth in nude mice (10). Down-regulation of the endogenous *Plk1* by using several antisense oligonucleotides targeted to *Plk1* induced growth inhibition in certain cancerous cells (31). Additionally, treatment of the cells with small interfering RNA targeted against *Plk1* caused the cell cycle arrest and apoptosis (32, 33). Of note, Liu and Erikson (33) reported that the tumor suppressor p53 might be involved in the Plk1 depletion-induced apoptosis. Recently, Plk1 has also been reported to have an ability to phosphorylate p53 *in vitro*, however, it is still unknown whether there exists a functional association between Plk1 and p53 (26). In sharp contrast to *Plk1*, the expression level of *Plk3* was significantly down-regulated in several human primary tumors including lung carcinomas and head and neck squamous cell carcinomas, as compared with their corresponding normal tissues (34, 35). Overexpression of Plk3 in mammalian cultured cells inhibited proliferation and induced apoptosis (36). Furthermore, it has been demonstrated that Plk3 physically interacts with p53 and phosphorylates the Ser^{20} of p53, which might result in the enhancement of its activity. These suggest that Plk1 and Plk3 play a differential role in regulating cell proliferation and oncogenesis, and that p53 participates in Plk3-dependent growth inhibition and/or apoptosis (25, 26, 36, 37).

In the present study, we examined the physical and functional interaction between Plk1 and p53. We found that Plk1 binds to the sequence-specific DNA-binding domain of p53, and inhibits the p53-dependent transcriptional activation as well as pro-apoptotic function. Intriguingly, overexpression of ATM abrogated the Plk1-mediated inhibitory effect on p53. These results suggest that the Plk1-mediated negative regulation of p53 might be a fundamental mechanism for the Plk1-induced oncogenesis.

EXPERIMENTAL PROCEDURES

Tumor Samples—Surgically resected tumor tissues including three lung adenocarcinomas, two gastric adenocarcinomas, one uterus carcinoma, two bladder carcinomas, and their corresponding normal tissues used in this study were obtained as frozen specimens from the Tissue Bank in Chiba Cancer Center Hospital (Chiba, Japan). Six hepatoblastomas and their matched normal tissues were provided by the Japanese Study Group for Pediatric Liver Tumor.

Cell Culture—African green monkey kidney COS7 cells were maintained in Dulbecco's modified Eagle's medium supplemented with 10% heat-inactivated fetal bovine serum (Invitrogen) and penicillin (100 IU/ml)/streptomycin (100 μg/ml). Human neuroblastoma SH-SY5Y cells and human lung carcinoma H1299 cells were grown in RPMI 1640 medium containing 10% heat-inactivated fetal bovine serum and antibiotic mixture. Cultures were maintained at 37 °C in a water-saturated atmosphere of 5% CO_2 in air.

Transfection—COS7 cells were transfected with the indicated expression plasmids using FuGENE 6 transfection reagent (Roche Applied Science) in a 6-cm diameter culture dish in accordance with the manufacturer's specifications. Transfection of H1299 cells was conducted by lipofection with LipofectAMINE transfection reagent (Invitrogen) in a 12-well plate according to the manufacturer's instructions.

RT-PCR—Total RNA was prepared from SH-SY5Y cells exposed to cisplatin by using the RNeasy Mini Kit (Qiagen Inc., Valencia, CA) according to the manufacturer's protocol, and subjected to synthesis of the first strand cDNA with random primers and a SuperScript II reverse transcriptase (Invitrogen) at 42 °C for 1 h. When the reaction was complete, the cDNA was amplified in a final volume of 15 μl of reaction mixture containing 100 μM of each deoxynucleoside triphosphate, 1× PCR buffer, 1 μM of each primer, and 0.2 units of rTaq DNA polymerase (Takara, Ohtsu, Japan). The primers for *p53* amplification were 5′-ATTTGATGCTGTCCCCGGACGATATTGAAC-3′ and 5′-ACCCTTTTTGGACTTCAGGTGGCTGGAGTG-3′. The primers for $p21^{WAF1}$ amplification were 5′-ATGAAATTCACCCCCTTTCC-3′ and 5′-CCCTAGGCTGTGCTCACTTC-3′. The primers for *Plk1* amplification were 5′-ATCACCTGCCTGACCATTCCACCAAGG-3′ and 5′-AATTGCGGAAATATTTAAGGAGGGTGATCT-3′. The primers for *Plk3* amplification were 5′-GCGCGAGAAGATCCTAAATG-3′ and 5′-GATCTGCCGCAGGTAGTAGC-3′. The primers for *GAPDH* amplification were 5′-ACCTGACCTGCCGTCTAGAA-3′ and 5′-TCCACCACCCTGTTGCTGTA-3′. The PCR-amplified products were separated by electrophoresis on a 1.5% agarose gel and visualized by ethidium bromide post-staining.

Generation of FLAG-tagged Expression Constructs—The FLAG-tagged human *Plk1* construct was generated by PCR amplification using the cDNA derived from primary hepatoblastoma as a template. The forward and reverse primers used in the PCR were 5′-CCGCTCGAGAGTGCTGCAGTGACTGCAGGGAAG-3′ and 5′-CTAGTCTAGATTAGGAGGCCTTGAGACGGTTGCT-3′. The underlined nucleotides represent the XhoI restriction sites in the forward primer and the XbaI restriction site in the reverse primer. The PCR product was subcloned into pGEM-T Easy (Promega Corp., Madison, WI), and its nucleotide sequence was verified by automated dideoxy terminator cycle sequencing. The PCR product was digested with XhoI and XbaI, and inserted between the XhoI to XbaI sites in the pcDNA3-FLAG expression plasmid in-frame to the downstream of the FLAG tag to give pcDNA3-FLAG-*Plk1*.

Construction of the Deletion Mutants of p53 and Plk1—The *p53* deletion mutants, *p53*-(1–359), *p53*-(1–292), and *p53*-(1–101) were generated by using the forward primer 5′-CCCAAGCTTGGGATGGAGGAGCCGCAGTCAGATCCTAGCGTC-3′ (1F) in combination with the reverse primers 5′-CCGGAATTCCGGTCATGGCTCCTTCCCAGCCTGGGCATCCTT-3′ (359R), 5′-CCGGAATTCCGGTCATTTCTTGCGGAGATTCTCTTCCTCTGT-3′ (292R) and 5′-CCGGAATTCCGGTCATTTCTGGGAAGGGACAGAAGATGACA-3′ (101R), respectively. *p53*-(102–393) was amplified by using the forward primer 5′-CCCAAGCTTGGGATGACCTACCAGGGCAGCTACGGTTTCCGTCT-3′ (102F) and the reverse primer 5′-CCGGAATTCCGGTCAGTCTGAGTCAGGCCCTTCTGTCTTGAACAT-3′ (393R). Each of the forward and reverse primers contained the HindIII and EcoRI restriction sites to facilitate the subsequent cloning step. Underlined nucleotides in the oligonucleotides listed above were HindIII or EcoRI sites. Amplified fragments were digested with HindIII and EcoRI, and subcloned directly into the identical restriction sites of pcDNA3 to give pcDNA3-*p53*-(1–359), pcDNA3-*p53*-(1–292), pcDNA3-*p53*-(1–101), and pcDNA3-*p53*-(102–393). All of the constructs were confirmed by sequence analysis. For the construction of the deletion mutants of Plk1, pcDNA3-FLAG-*Plk1* was digested with BamHI, BamHI and BstXI, or BamHI and NcoI. A restriction fragment encoding amino acid residues 1–401, 1–329, or 1–98 was purified from agarose gels, filled in the overhangs with Klenow, and then inserted in-frame into the enzymatically modified BamHI and XhoI sites of the pcDNA3-FLAG expression plasmid to give pcDNA3-FLAG-*Plk1*-(1–401), pcDNA3-FLAG-*Plk1*-(1–329), or pcDNA3-FLAG-*Plk1*-(1–98), respectively. DNA sequencing confirmed the authenticity of the expression plasmids prior to transfection.

Construction of the Kinase-deficient Mutant Form of Plk1—The K82M mutation was introduced into wild-type Plk1 by the PCR-based strategy using *PfuUltra*™ High Fidelity DNA polymerase (Stratagene, La Jolla, CA) according to the manufacturer's instructions. The following oligonucleotides were used: 5′-ATGATTGTGCCTAAGTCTCTGCTGCTCAAGCCGCA-3′ (underlined segment encodes Met at amino acid position 82) and 5′-GCCCGCGAACACCTCCTTGGTGTCCGCGTCCGAGA-3′. Nucleic acid sequencing was performed to verify the presence of the desired mutation and absence of random mutations. The amplified fragment that contains the K82M mutation was then digested with HindIII and NcoI, gel-purified, and ligated with the NcoI/XbaI restriction fragment containing the 3′-portion of the wild-type *Plk1* cDNA. The resulting entire cDNA encoding the full-length Plk1 carrying the amino acid substitution at position 82 was inserted in-frame into the HindIII and XbaI sites of the pcDNA3-FLAG expression plasmid to give pcDNA3-FLAG-*Plk1*(K82M).

Construction of the Expression Plasmid for Antisense Plk1—A full-length human *Plk1* cDNA was ligated into the pcDNA3 expression plasmid in a reverse orientation to give As-*Plk1*, and the product was evaluated by restriction digestion. To assess the effect of As-*Plk1* on the endogenous Plk1, whole cell lysates prepared from H1299 cells transfected with As-*Plk1* were analyzed for Plk1 by immunoblotting.

GST Pull-down Assay—Whole cell lysates prepared from COS7 cells expressing FLAG-Plk1 were incubated with 1 μg of GST or GST-p53 (Santa Cruz Biotechnologies, Santa Cruz, CA) immobilized on glutathione-Sepharose beads for 2 h at 4 °C. The beads were washed extensively with NETN buffer (50 mM Tris-Cl, pH 7.5, 150 mM NaCl, 0.1% Nonidet P-40, and 1 mM EDTA) containing 1 mM phenylmethylsulfonyl fluoride. The bound proteins were eluted with 2× SDS sample buffer by boiling

for 5 min, and separated by 10% SDS-polyacrylamide gel electrophoresis followed by immunoblotting.

Immunofluorescent Labeling and Confocal Microscopy—COS7 cells, cultured onto glass coverslips, were transiently transfected with the expression plasmid for FLAG-Plk1. Transfected cells were washed twice with 1× PBS and then fixed with 1× PBS containing 3.7% formaldehyde for 30 min at room temperature. After washing with 1× PBS, cells were permeabilized with 0.2% Triton X-100 for 5 min at room temperature and blocked for 1 h in 1× PBS containing 3% bovine serum albumin. Cells were then incubated with polyclonal anti-p53 antibody (Cell Signaling Technology, Inc., Beverly, MA) and monoclonal anti-FLAG antibody (M2, Sigma) for 1 h at room temperature. After incubation with primary antibodies, cells were washed twice with 1× PBS and incubated with fluorescein isothiocyanate- or rhodamine-conjugated secondary antibodies (Invitrogen) diluted 1:200 for 1 h at room temperature. Cell nuclei were stained with 4,6-diamidino-2-phenylindole at a final concentration of 1 μg/ml (Sigma). Cells were finally washed with 1× PBS, the coverslips were removed from the dishes, mounted onto slides, and observed under Fluoview laser scanning confocal microscope (Olympus, Tokyo, Japan).

Western Blot Analysis—Cells were transfected with the indicated combinations of the expression plasmids. Forty-eight hours after transfection, cells were extracted directly with the lysis buffer containing 25 mM Tris-HCl, pH 8.0, 137 mM NaCl, 2.7 mM KCl, 1% Triton X-100, 1 mM phenylmethylsulfonyl fluoride and protease inhibitor mixture (Sigma) and the whole cell lysates were sonicated for 10 s followed by centrifugation at 15,000 rpm for 10 min at 4 °C to remove insoluble materials. The protein concentrations were determined using the Bradford protein assay according to the instructions of the vendor (Bio-Rad). Equal amounts of the whole cell lysates (50 μg of protein) were boiled in an SDS sample buffer consisting of 62.5 mM Tris-HCl, pH 6.8, 2% SDS, 2% β-mercaptoethanol, and 0.01% bromphenol blue and subjected to 10% SDS-polyacrylamide gel electrophoresis under reducing conditions and then electrotransferred onto Immobilon-P membranes (Millipore, Bedford, MA) at room temperature for 1 h. The membranes were blocked with TBS-T (50 mM Tris-Cl, pH 7.6, 100 mM NaCl, and 0.1% Tween 20) containing 5% nonfat dry milk at room temperature for 1 h, and subsequently incubated for 1 h with monoclonal anti-Plk1 (PL2 and PL6, Zymed Laboratories, Inc., San Francisco, CA), monoclonal anti-p53 (DO-1, Oncogene Research Products, Cambridge, MA), monoclonal anti-FLAG antibody (M2, Sigma), monoclonal anti-Plk3 antibody (B37–2, BD Pharmingen), polyclonal antibody specific for p53 phosphorylated at Ser^{15} (Cell Signaling, Beverly, MA), polyclonal anti-$p21^{WAF1}$ antibody (H-164, Santa Cruz Biotechnologies), or polyclonal anti-actin antibody (20–33, Sigma) in TBS-T, followed by an incubation with horseradish peroxidase-conjugated goat anti-mouse or anti-rabbit secondary antibody (Jackson ImmunoResearch Laboratories, West Grove, PA) diluted at 1:2,000 for 1 h at room temperature. The membranes were washed extensively with TBS-T and protein bands were visualized by enhanced chemiluminescence (ECL) according to the manufacturer's instructions (Amersham Biosciences).

Subcellular Fractionation—Cells were fractionated into cytosolic and nuclear fractions as described previously (38). Briefly, cells were washed twice with ice-cold 1× PBS and lysed in lysis buffer containing 10 mM Tris-HCl, pH 7.5, 1 mM EDTA, 0.5% Nonidet P-40, and a protease inhibitor mixture (Sigma) for 30 min at 4 °C. Cell lysates were centrifuged at 15,000 × *g* for 10 min to collect the soluble fraction as cytosolic extracts. Insoluble materials were washed with the lysis buffer and further dissolved in 1× SDS sample buffer to collect the nuclear fraction. The nuclear and cytoplasmic fractions were subjected to immunoblot analysis using the anti-FLAG, monoclonal anti-lamin B (Ab-1, Oncogene Research Products), or monoclonal anti-Ras (RASK-3, Seikagaku Co., Tokyo, Japan) antibody.

Immunoprecipitation and Western Blot Analysis—For the immunoprecipitation of Plk1 and p53, COS7 cells were transiently transfected with 2 μg of the expression plasmid for FLAG-Plk1 using FuGENE 6 transfection reagent. Forty-eight hours post-transfection, cells were harvested and lysed by incubation with mixing in 400 μl of the EBC buffer (50 mM Tris-HCl, pH 7.5, 120 mM NaCl, 0.5% Nonidet P-40, and 1 mM phenylmethylsulfonyl fluoride) at 4 °C for 30 min. Whole cell lysates were then subjected to centrifugation at 15,000 × *g* for 20 min at 4 °C to remove insoluble materials. Equal amounts of whole cell lysates were precleared with 30 μl of a 50% slurry of protein A-Sepharose (Amersham Biosciences). After centrifugation, the supernatant was incubated with the normal mouse serum (NMS), monoclonal anti-FLAG, or monoclonal anti-p53 antibody at 4 °C for 2 h. The immunocomplexes were precipitated with the protein A-Sepharose beads at 4 °C for 30 min, which were then pelleted by centrifugation at 15,000 × *g* for 5 min. The precipitates were washed with the lysis buffer three times at 4 °C, resuspended in 30 μl of the SDS sample buffer, and treated at 100 °C for 5 min. Proteins were then resolved by 10% SDS-polyacrylamide gel electrophoresis, and transferred onto the Immobilon-P membranes. The protein complex was detected by Western blot analysis using the monoclonal anti-FLAG or monoclonal anti-p53 antibodies.

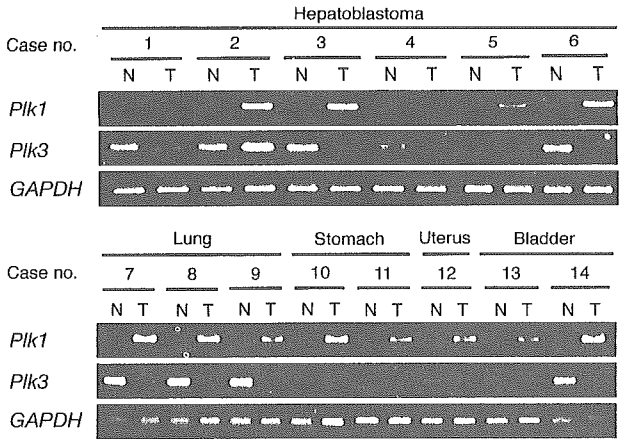

FIG. 1. **Expression of *Plk1* and *Plk3* mRNA in various human primary tumors and their corresponding normal tissues.** Total RNA (5 μg) prepared from the indicated tumor (*T*)-normal (*N*) paired samples was subjected to RT-PCR analysis for *Plk1* and *Plk3* mRNA expression using the specific primers as shown under "Experimental Procedures." The PCR-amplified products were analyzed by 1.5% agarose gel electrophoresis and visualized by ethidium bromide staining. Amplification of *GAPDH* was used as an internal control.

Luciferase Reporter Assays—p53-deficient H1299 cells were seeded in a 12-well tissue culture dish at a density of 5×10^4 cells/well. Cells were transfected with 100 ng of the p53-responsive luciferase reporter plasmid (*p21*, *MDM2*, or *BAX*), 10 ng of pRL-TK *Renilla* luciferase cDNA, and 25 ng of the expression plasmid for p53 together with or without increasing amounts of FLAG-Plk1 expression plasmid. The total amount of DNA was kept constant (510 ng) with pcDNA3 (Invitrogen) per transfection. Forty-eight hours post-transfection, transfected cells were washed twice with 1× PBS, and resuspended in passive lysis buffer (Promega Corp.). Both firefly and *Renilla* luciferase activities were assayed with the dual-luciferase reporter assay system (Promega Corp.) according to the manufacturer's instructions. The fluorescent light emission was determined by TD-20 luminometer (Turner Design, Sunnylvale, CA). The firefly luminescence signal was normalized based on the *Renilla* luminescence signal. The results were obtained from at least three sets of transfection and were presented as the mean ± S.D.

Cell Survival Assays—Cell viability was determined by a modified 3-(4,5-dimethylthiazol-2-yl)-2,5-diphenyltetrazolium bromide (MTT) assay. In brief, SH-SY5Y cells were seeded in 96-well microtiter plates (5×10^3 cell/well) with 100 μl of complete medium and allowed to attach. The next day, the medium were changed and cells were treated with cisplatin for 24 h. For the MTT assay, 10 μl of MTT solution was added to each well for 3 h at 37 °C. The absorbance readings for each well were carried out at 570 nm using the microplate reader (model 450, Bio-Rad).

Apoptotic Analysis—H1299 cells were transfected with a constant amount of the expression plasmid for green fluorescence protein (GFP) and p53 expression plasmid together with or without the expression plasmid encoding FLAG-Plk1. Forty-eight hours after transfection, transfected cells were identified by the presence of green fluorescence. To verify apoptosis, cell nucleus was stained with propidium iodide to reveal nuclear condensation and fragmentation. The number of GFP-positive cells with fragmented nuclei was scored, and presented as a percentage of the total number of fluorescent cells.

RESULTS

Expression of Plk1 and Plk3 in Paired Tumors and Adjacent Normal Tissues—It has been shown that the expression level of *Plk1* is increased in human tumors of various origins as compared with that of their corresponding normal tissues, suggesting that Plk1 contributes to the genesis and/or progression of tumors (13, 27–29). Recently, we have also identified *Plk1* as

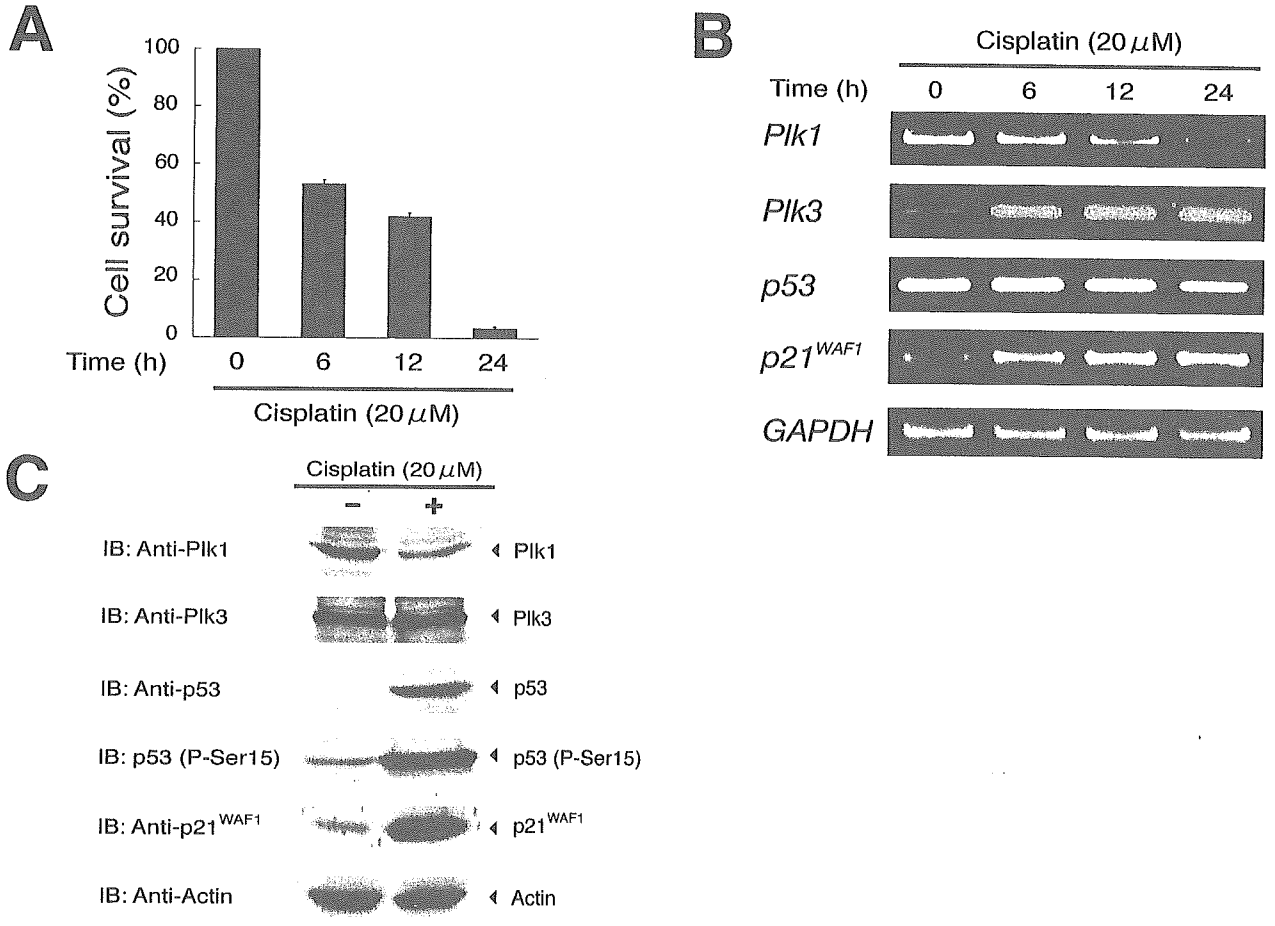

FIG. 2. **Down-regulation of *Plk1* during the cisplatin-induced apoptosis.** *A*, cell survival assays of SH-SY5Y cells treated with cisplatin. SH-SY5Y cells were exposed to cisplatin at a final concentration of 20 μM. At the indicated time periods after treatment with cisplatin, cell viability was determined by MTT assay. Data are presented as the mean ± S.D. of three independent experiments. *B*, RT-PCR analysis. Human neuroblastoma-derived SH-SY5Y cells were treated with or without cisplatin at a final concentration of 20 μM. At the indicated time periods after treatment with cisplatin, total RNA was prepared and subjected to RT-PCR analysis for the expression of *Plk1* (*1st panel*), *Plk3* (*2nd panel*), *p53* (*3rd panel*), and *p21*^{WAF1} (*4th panel*). Amplification of *GAPDH* serves as an internal control (*5th panel*). The PCR products were resolved in 1.5% agarose gels and visualized by ethidium bromide staining. *C*, Western blot analysis. Whole cell lysates were prepared from SH-SY5Y cells exposed to cisplatin for 24 h (at a final concentration of 20 μM) or left untreated and immunoblotted against anti-Plk1 (*1st panel*), anti-Plk3 (*2nd panel*), anti-p53 (*3rd panel*), antibody specific for p53 phosphorylated at Ser^{15} (*4th panel*), or with the anti-p21^{WAF1} antibody (*5th panel*). Immunoblotting for actin is shown as control for protein loading (*6th panel*).

one of the genes whose expression level is markedly elevated in human hepatoblastomas.[2] In contrast, *Plk3* expression is down-regulated in certain human tumors including lung carcinomas and head and neck squamous cell carcinomas (34, 35). To confirm the differential expression of both *Plk1* and *Plk3* in the same tissue samples, we examined their expression patterns among the indicated various paired cancer-normal tissues by RT-PCR. The levels of *GAPDH* mRNA were comparable between these paired samples. Consistent with the previous results, without exceptions, the expression levels of *Plk1* mRNA were significantly higher in cancerous tissues than those of their adjacent normal tissues (Fig. 1). On the other hand, *Plk3* was expressed at low levels in all the lung, uterus, and bladder carcinomas that we examined, as compared with their corresponding normal tissues, whereas a significant decrease in *Plk3* expression level in tumor tissues was undetectable in 2 of 6 hepatoblastomas and in 1 of 2 gastric carcinomas (Fig. 1). Thus, deregulated overexpression of *Plk1* is detected in all various types of tumors, whereas down-regulation of *Plk3* expression may be restricted to certain tumors.

[2] Yamada, S., Ohira, M., Horie, H., Ando, K., Takayasu, H., Suzuki, Y., Sugano, S., Hirata, T., Goto, T., Matsunaga, T., Hiyama, E., Hayashi, Y., Ando, H., Suita, S., Kaneko, M., Sakaki, F., Hashizume, K., Ohnuma, N., and Nakagawara, A. (2004) *Oncogene*, in press.

Cisplatin Treatment Induces Down-regulation of Plk1 in Association with Up-regulation of p53 in SH-SY5Y Cells—To analyze whether Plk1 expression could be modulated during the cisplatin-induced apoptosis, whole cell lysates and total RNA were prepared from human neuroblastoma-derived SH-SY5Y cells after treatment with or without cisplatin, and were subjected to immunoblot analysis and RT-PCR, respectively. In accordance with our previous observations (39), cells underwent apoptosis in a time-dependent manner as measured by the cell survival assay (Fig. 2*A*), and a remarkable stabilization of p53 at the protein level was detected after treating the cells with cisplatin, accompanied with a significant up-regulation of p21^{WAF1} both at protein and mRNA levels (Fig. 2, *B* and *C*). In addition to the increase in the level of total p53, the phosphorylation of p53 at Ser^{15} was dramatically enhanced in cells exposed to cisplatin, whereas that of p53 at Ser^{20} was undetectable (data not shown). Intriguingly, cisplatin treatment markedly reduced the expression level of *Plk1* mRNA and protein (Fig. 2, *B* and *C*), suggesting that there exists an inverse relationship between the expression levels of p53 and Plk1 during DNA damage-induced apoptosis. Thus, Plk1 may play an important role in the p53 pathway. On the other hand, cisplatin treatment resulted in a significant up-regulation of *Plk3* mRNA expression in a time-dependent manner, however,

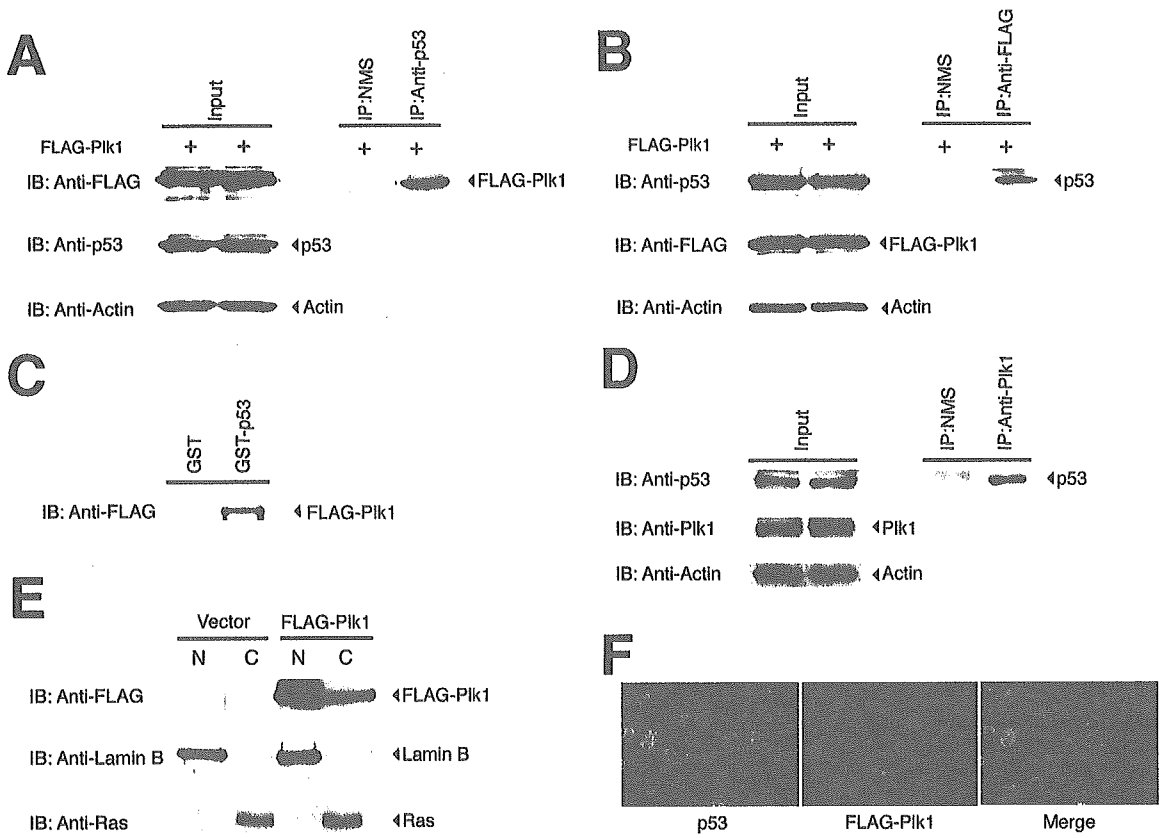

FIG. 3. **Co-immunoprecipitation and nuclear co-localization of Plk1 and p53.** *A*, complex formation between Plk1 and p53 in mammalian cultured cells. COS7 cells were transiently transfected with the expression plasmid for FLAG-tagged Plk1. Forty-eight hours after transfection, whole cell lysates were prepared and immunoprecipitated (*IP*) with NMS or with monoclonal anti-p53 antibodies. The immunocomplexes were resolved by 10% SDS-polyacrylamide gel electrophoresis and immunoblotted (*IB*) with monoclonal anti-FLAG antibody. Whole cell lysates were immunoblotted with monoclonal anti-p53, or with monoclonal anti-FLAG antibody to show the expression of endogenous p53, or FLAG-Plk1, respectively. The p53 blot was reprobed for actin to ensure equal loading. *B*, a similar immunoprecipitation assay was performed with NMS or monoclonal anti-FLAG antibody, followed by immunoblotting with monoclonal anti-p53 antibody. Whole cell lysates were monitored on immunoblot for the expression of endogenous p53 or FLAG-Plk1. The p53 blot was reprobed for actin to ensure equal loading. *C*, GST pull-down assay. Whole cell lysates prepared from COS7 cells expressing FLAG-Plk1 were incubated with GST or GST-p53 immobilized on glutathione-Sepharose beads. The bound proteins were separated by 10% SDS-polyacrylamide gel electrophoresis, and subjected to immunoblotting with the anti-FLAG antibody. *D*, association between endogenous p53 and Plk1. Cell lysates prepared from U2OS cells were immunoprecipitated with NMS or with monoclonal anti-Plk1 antibody, and the anti-Plk1 immunoprecipitates were immunoblotted with monoclonal anti-p53 antibody. *E*, subcellular localization of Plk1. COS7 cells were transiently transfected with the expression plasmid encoding FLAG-Plk1. Forty-eight hours after transfection, cells were fractionated into nuclear (*N*) and cytosolic (*C*) fractions as described under "Experimental Procedures." Equal amounts of each fraction were resolved by 10% SDS-polyacrylamide gel electrophoresis and immunoblotted with monoclonal anti-FLAG antibody (*top panel*). These extracts were also immunoblotted with monoclonal antibody specific for lamin B (*middle panel*) or Ras (RASK-3) (*bottom panel*) to show the validity of our fractionation technique. *F*, nuclear co-localization of Plk1 and p53. COS7 cells were transiently transfected with the FLAG-Plk1 expression plasmid. Following transfection, cells were fixed and incubated with polyclonal anti-p53 and monoclonal anti-FLAG antibodies that were revealed by fluorescein isothiocyanate-conjugated anti-rabbit IgG (*green*) and rhodamine-conjugated anti-mouse IgG (*red*), respectively. Merge analysis (*yellow*) showed the nuclear co-localization of Plk1 and p53.

the amount of Plk3 protein remained constant, regardless of cisplatin treatment.

Interaction of Plk1 with p53—Recently, it has been shown that Plk3 interacts with p53 and is directly involved in the stress-induced phosphorylation of p53 on the serine 20 residue (25, 26, 36, 37). Of note, Xie *et al.* (26) found that Plk1 is able to phosphorylate p53 *in vitro*, however, its functional significance *in vivo* remains unclear. These observations prompted us to investigate possible interactions between Plk1 and p53. For this purpose, COS7 cells, which express a large amount of endogenous p53 (40), were transiently transfected with the expression plasmid for FLAG-tagged Plk1. Whole cell lysates prepared from the transfected cells were immunoprecipitated with NMS or with a monoclonal anti-p53 antibody, and the immunoprecipitates were analyzed by immunoblotting with a monoclonal anti-FLAG antibody. As shown in Fig. 3*A*, FLAG-Plk1 was co-immunoprecipitated with the endogenous p53, but not present in the control immunoprecipitates obtained with the normal mouse serum. The expression of FLAG-Plk1 and the endogenous p53 was confirmed by immunoblot analysis with the antibody against the FLAG epitope and p53, respectively (Fig. 3*A*). Analysis of the anti-FLAG immunoprecipitates also revealed that p53 is co-immunoprecipitated with FLAG-Plk1 (Fig. 3*B*). To confirm their interaction *in vitro*, GST pull-down experiments were performed using GST fusion full-length human p53. As shown in Fig. 3*C*, mammalian expressed FLAG-Plk1 bound to GST-p53 but not to GST alone. Their interaction was further examined using endogenous materials. Whole cell lysates prepared from U2OS cells that carry wild-type p53 (41) were immunoprecipitated with a monoclonal anti-Plk1 antibody and the anti-Plk1 immunoprecipitates were analyzed for the presence of the endogenous p53. As shown in Fig. 3*D*, the endogenous p53 was co-immunoprecipitated with the endogenous Plk1. Similar results were also obtained in HeLa cells (data not shown). These results clearly demonstrate that Plk1 interacts with p53 in mammalian cultured cells and *in vitro*.

To evaluate the subcellular localization of Plk1, we per-

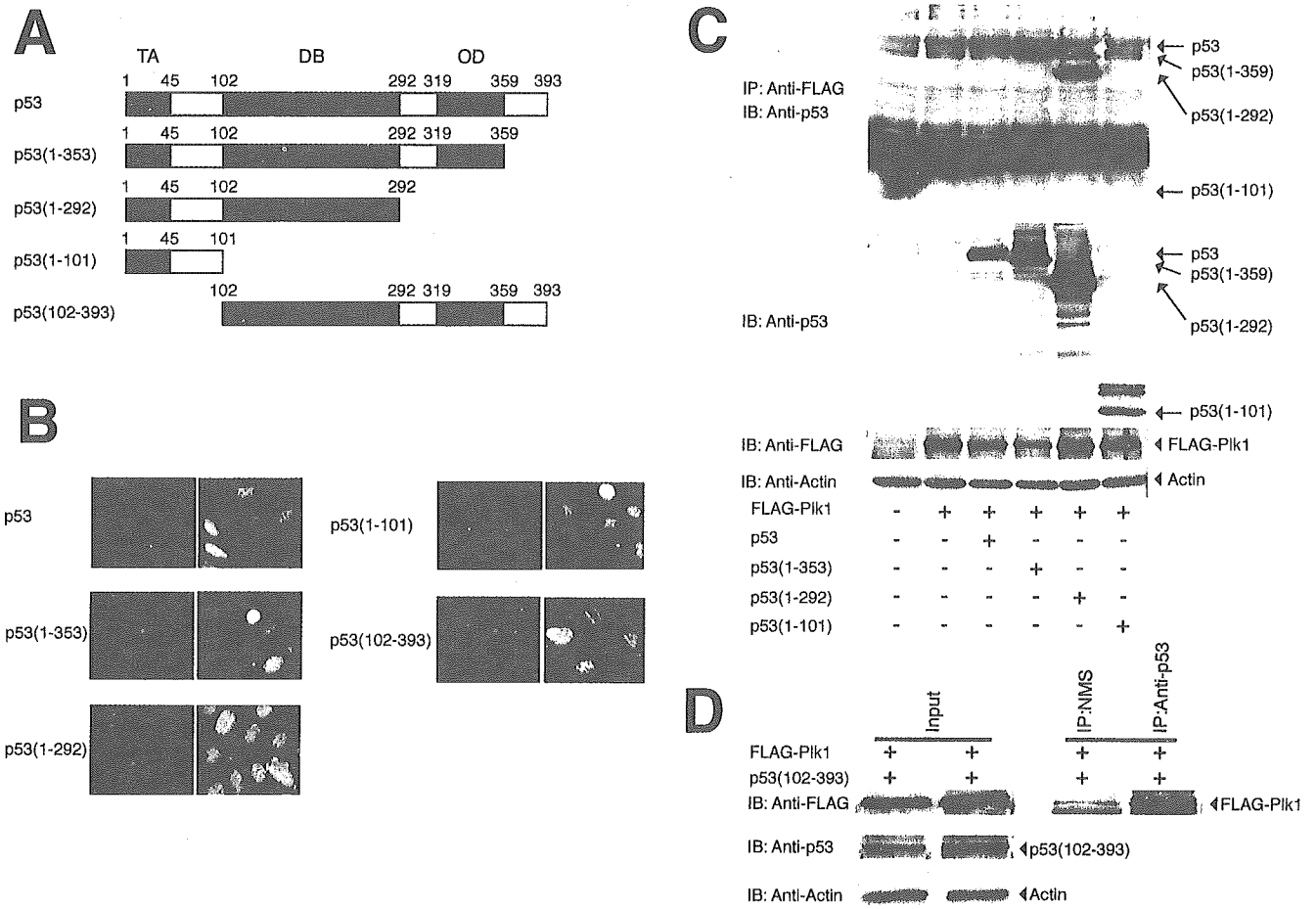

FIG. 4. **DNA-binding domain of p53 is required for interaction with Plk1.** *A*, schematic drawing of full-length p53 and various deletion mutants used in this study. *TA*, transactivation domain; *DB*, sequence-specific DNA-binding domain; *OD*, oligomerization domain. *Numbers* indicate amino acid position. *B*, subcellular localization of various deletion mutants of p53. *p53*-deficient H1299 cells were transiently transfected with the indicated expression plasmids. Forty-eight hours after transfection, cells were fixed and incubated with monoclonal anti-p53 antibody (DO-1 or PAb 421). Cell nuclei were stained with 4,6-diamidino-2-phenylindole (*blue*). Expression of p53 derivatives was visualized with rhodamine-conjugated secondary antibody (*red*). *C* and *D*, Plk1 interacts with the DNA-binding domain of p53. H1299 cells were transiently co-transfected with the indicated combinations of the expression plasmids. Forty-eight hours after transfection, whole cell lysates were prepared and subjected to immunoprecipitation with monoclonal anti-FLAG antibody followed by immunoblotting with monoclonal anti-p53 antibody (*upper panel*). The *lower panels* show the direct immunoblot analyses of whole cell lysates performed with monoclonal anti-p53, monoclonal anti-FLAG, or with polyclonal anti-actin antibody (*C*). Whole cell lysates from H1299 cells overexpressing FLAG-Plk1 and p53-(102–393) were immunoprecipitated with monoclonal anti-p53 antibody (PAb421) or with NMS followed by immunoblotting with monoclonal anti-FLAG antibody. Expression levels of p53-(102–393), FLAG-Plk1, and actin were examined by immunoblotting (*D*).

formed indirect immunofluorescent staining as well as biochemical cell fractionation of the transfected COS7 cells. COS7 cells transfected with the empty plasmid or with the expression plasmid for FLAG-Plk1 were fractionated into cytoplasmic and nuclear fractions for immunoblot analysis of FLAG-Plk1. Ras and lamin B served as markers for the purity of cytoplasmic and nuclear fractions, respectively (Fig. 3*E*, *lower panels*). Consistent with previous observations (10, 22, 42), FLAG-Plk1 was detected both in the cytoplasm and nucleus (Fig. 3*E*, *upper panel*). For immunofluorescent staining, COS7 cells expressing FLAG-Plk1 were fixed and stained with monoclonal anti-FLAG and polyclonal anti-p53 antibodies. As shown in Fig. 3*F*, FLAG-Plk1 localized to both the cytoplasm and nucleus. Merging analysis by confocal microscopy showed that FLAG-Plk1 co-localizes with endogenous p53 in cell nucleus.

The Sequence-specific DNA-binding Region of p53 Is Required for the Interaction with Plk1—To assess regions of p53 involved in the interaction with Plk1, we constructed a series of p53 deletion mutants including p53-(1–359) (lacking an extreme COOH-terminal region), p53-(1–292) (lacking the most COOH-terminal region including an oligomerization domain), p53-(1–101) (retaining only an NH_2-terminal transactivation domain), and p53-(102–393) (lacking an NH_2-terminal transactivation domain) (Fig. 4*A*). We first examined their subcellular localization by indirect immunofluorescent staining. To this end, p53-deficient human lung carcinoma H1299 cells (43) were transiently transfected with each expression plasmid. Forty-eight hours after transfection, cells were fixed and stained with the appropriate monoclonal anti-p53 antibody. As described previously (44, 45), there exist three potential nuclear localization signals (NLS I, II, and III) in the COOH-terminal region of p53, and NLS I alone has an ability to translocate the pyruvate kinase fusion protein to the nucleus. As shown in Fig. 4*B*, wild-type p53 and p53-(102–393), which retain the intact COOH-terminal region, accumulated in the nucleus. In addition, p53-(1–359), which lacks the NLS II and III but retains the NLS I, localized largely in the nucleus. On the other hand, p53-(1–292) and p53-(1–101), which lack three potential NLSs, were detected both in the nucleus and the cytoplasm. We then examined their abilities to interact with Plk1. H1299 cells were transiently co-transfected with the FLAG-Plk1 expression plasmid along with the expression plasmid for wild-type p53, p53-(1–359), p53-(1–292), or p53-(1–101), and the anti-FLAG immunoprecipitates were analyzed for the presence of wild-

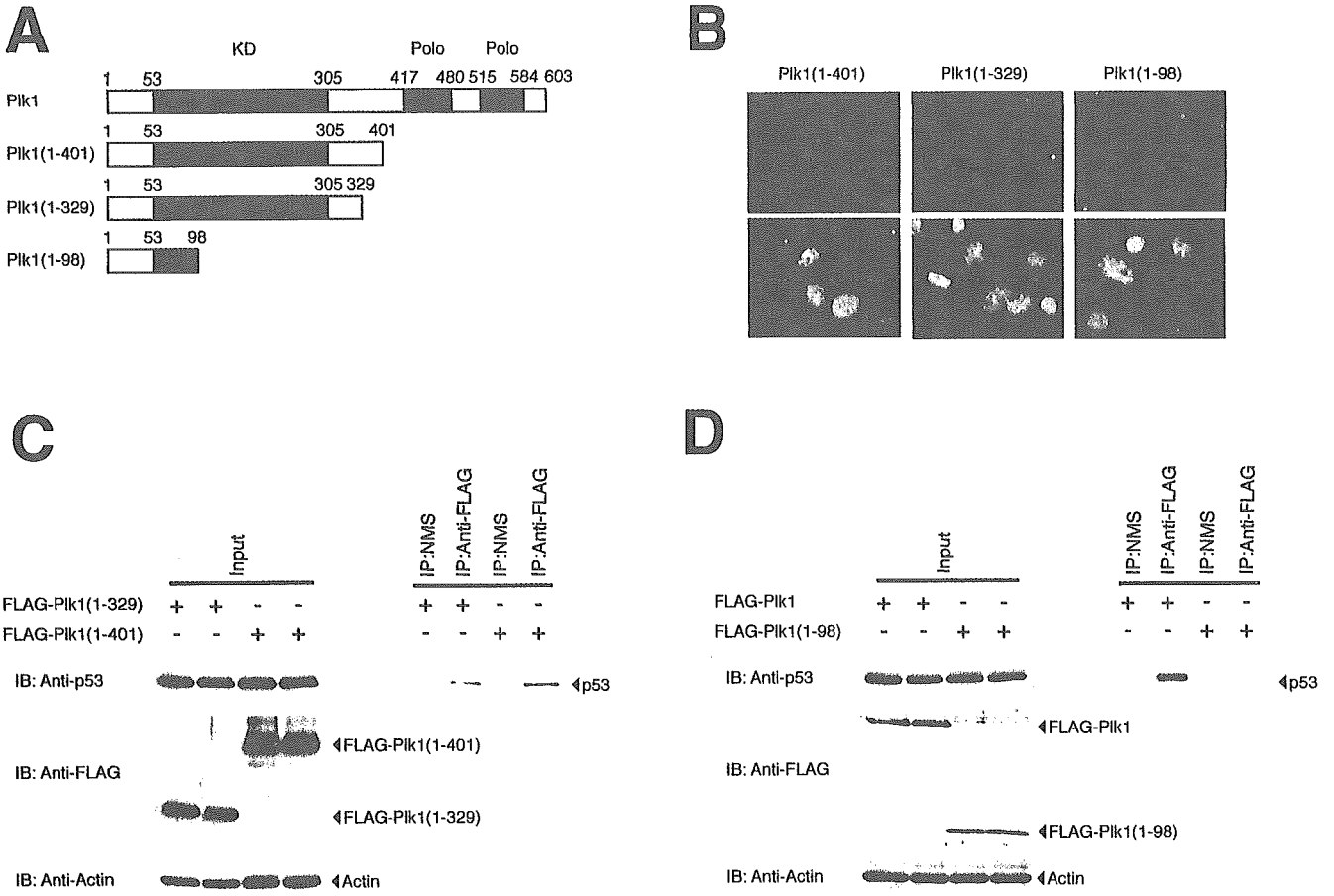

FIG. 5. **Mapping of the region of Plk1 required for interaction with p53.** *A*, schematic representation of Plk1 deletion mutants. *KD*, kinase domain; *Polo*, polo-box. *Numbers* indicate amino acid position. *B*, immunofluorescent studies of Plk1 deletion mutants. Transfected COS7 cells were fixed in 3.7% formaldehyde for 30 min, permeabilized with 0.2% Triton X-100 for 5 min, and blocked in PBS containing 3% bovine serum albumin for 1 h. Cells were then incubated with monoclonal anti-FLAG antibody followed by incubation with rhodamine-conjugated secondary antibody (*red*), and analyzed by confocal microscopy. Cell nuclei were stained with 4,6-diamidino-2-phenylindole (*blue*). *C* and *D*, interaction between various Plk1 deletion mutants and endogenous p53. Whole cell lysates from COS7 cells transfected with the indicated expression plasmids were immunoprecipitated with monoclonal anti-FLAG antibody, and immunoblotted with monoclonal anti-p53 antibody to observe the interaction between Plk1 deletion mutants and p53. Immunoprecipitation with NMS was used as a negative control. Equal amounts of protein derived from cell lysates were immunoblotted with monoclonal anti-p53, monoclonal anti-FLAG, or polyclonal anti-actin antibody.

type p53 and these truncated forms of p53. As shown in Fig. 4*C*, wild-type p53 as well as p53 deletion mutants including p53-(1–359) and p53-(1–292), were detected in the anti-FLAG immunoprecipitates, whereas p53-(1–101) has lost the ability to bind to Plk1, indicating that the extreme COOH-terminal region, the oligomerization domain, and the NH_2-terminal transactivation domain of p53 are not involved in the interaction with Plk1. Similar immunoprecipitation analyses revealed that p53-(102–393) co-precipitates with FLAG-Plk1 (Fig. 4*D*). Thus, the region between amino acid residues 102 and 292 of p53, which includes the sequence-specific DNA-binding domain, appears to be required and sufficient for the interaction with Plk1.

Mapping of the p53-binding Region of Plk1—To map the p53-interacting domain on Plk1, we have constructed the FLAG-tagged Plk1 deletion mutants including Plk1-(1–401), Plk1-(1–329), and Plk1-(1–98) (Fig. 5*A*), and examined their subcellular localization by indirect immunofluorescent staining. As shown in Fig. 5*B*, COS7 cells transfected with each of the expression plasmids for FLAG-tagged Plk1 deletion mutants exhibited intense staining of the nucleus. Inspection of the amino acid sequence of Plk1-(1–98) identified one cluster of basic amino acids (^{48}RSRRRYVRGR^{57}), suggesting that this basic cluster acts as a nuclear localization signal. We then tested the interaction between p53 and each of these Plk1 deletion mutants. COS7 cells were transfected with the expression plasmid encoding Plk1-(1–401), Plk1-(1–329), or Plk1-(1–98), and co-immunoprecipitation experiments were performed to determine the interaction. We found that Plk1-(1–401) and Plk1-(1–329) retained the ability to bind to p53, whereas Plk1-(1–98) did not (Fig. 5*C*). These results indicate that the amino acid sequence comprising residues 99 to 329 of Plk1 contains the p53-binding domain.

Plk1 Inhibits the p53-mediated Transcriptional Activation—To determine whether Plk1 could affect the transcriptional activity of p53, H1299 cells were transiently co-transfected with a constant amount of the expression plasmid encoding p53 together with the p53-responsive *p21^{WAF1}*, *MDM2*, or *BAX*-luciferase reporter constructs in the presence or absence of increasing amounts of the expression plasmid for FLAG-Plk1. Under our experimental conditions, ectopically expressed p53 successfully activated the transcription of each of those p53-responsive reporters as compared with the empty plasmid controls, but Plk1 alone had no effect on luciferase activity (Fig. 6). Expression of FLAG-Plk1 greatly reduced the ability of p53 to increase the *p21^{WAF1}*-, *MDM2*-, and *BAX*-luciferase activities in a dose-dependent manner (Fig. 6, *A–C*). In addition, Plk1-(1–98), which lacks an ability to interact with p53, did not affect the p53 transcriptional activity toward the *p21^{WAF1}*, *MDM2*, and *BAX* promoters (data not shown). To confirm the inhibitory role of Plk1 in the p53-mediated transactivation, we assayed H1299 cell transfectants for induction of the endoge-

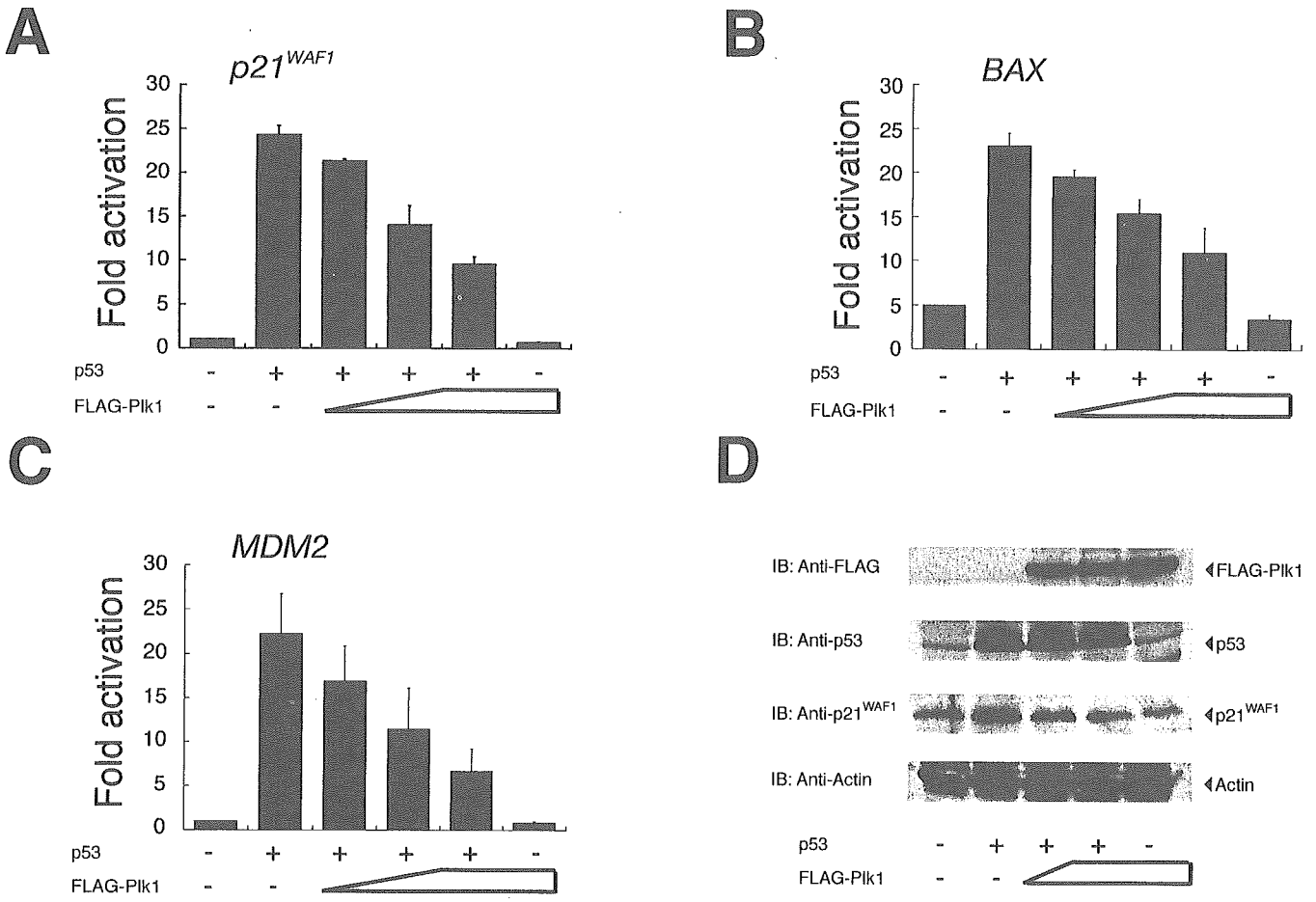

FIG. 6. **Plk1 abrogates the p53-mediated transcriptional activation.** *p53*-deficient H1299 cells (5×10^4 cells/well) were transiently co-transfected with 25 ng of the expression plasmid for p53 together with 100 ng of the luciferase reporter construct that carries the p53-responsive element derived from $p21^{WAF1}$ (*A*), *BAX* (*B*), or *MDM2* (*C*) promoter and 10 ng of the *Renilla* luciferase plasmid (pRL-TK) in the presence or absence of increasing amounts of pcDNA3-FLAG-Plk1 (50, 100, or 200 ng). The total amount of plasmid DNA per transfection was kept constant (510 ng) with pcDNA3. All transfections were performed in triplicate. Forty-eight hours after transfection, cells were lysed, and analyzed for their luciferase activities. Firefly luminescence signal was normalized based on the *Renilla* luminescence signal. Results are shown as -fold induction of the firefly luciferase activity compared with control cells transfected with pcDNA3 alone. *D*, immunoblot analysis. H1299 cells were transiently co-transfected with the indicated combinations of expression plasmids. Whole cell lysates were prepared 48 h post-transfection, and analyzed for the expression of FLAG-Plk1 (*1st panel*), p53 (*2nd panel*), or $p21^{WAF1}$ (*3rd panel*) by immunoblot analysis with monoclonal anti-FLAG, monoclonal anti-p53, or polyclonal anti-$p21^{WAF1}$ antibody, respectively. Total protein levels were controlled with polyclonal anti-actin antibody (*4th panel*).

nous $p21^{WAF1}$. To this end, H1299 cells were transiently co-transfected with a constant amount of the expression plasmid for p53 together with or without increasing amounts of the FLAG-Plk1 expression plasmid. Forty-eight hours after transfection, whole cell lysates were prepared and subjected to immunoblot analysis. Equal protein loading was confirmed by immunoblotting with the antibody against actin. As described (46), overexpression of p53 in H1299 cells resulted in the induction of the endogenous $p21^{WAF1}$ compared with basal levels seen with empty plasmid (Fig. 6*D*, *first* and *second lanes*). Co-expression of p53 with FLAG-Plk1 caused a significant decrease in the endogenous $p21^{WAF1}$ level in a dose-dependent manner (Fig. 6*D*, *third* and *fourth lanes*). These findings strongly suggest that Plk1 has an ability to inhibit p53-mediated transcriptional activation through physical interaction with p53.

To assess the possible effect of the endogenous Plk1 on the transcriptional activity of p53, we have employed an antisense strategy. As shown in Fig. 7*A*, expression of antisense *Plk1* in H1299 cells resulted in a reduction of the endogenous Plk1 as detected by immunoblot analysis. We then performed luciferase reporter analysis utilizing H1299 cells. As expected, co-expression of p53 with the antisense *Plk1* led to a slight but significant increase in the p53-mediated transcriptional activation as compared with cells expressing p53 alone (Fig. 7, *B–D*).

Plk1 Inhibits the p53-mediated Apoptosis—To extend the functional significance of the physical interaction between Plk1 and p53, we next determined whether Plk1 could affect p53-mediated apoptosis. H1299 cells were transiently co-transfected with the expression plasmid encoding p53 together with or without the expression plasmid for FLAG-Plk1. Forty-eight hours after transfection, cell viability was monitored by a cell survival assay. As shown in Fig. 8*A*, overexpression of p53 resulted in a reduction of the number of viable cells as compared with that found in the control transfection, and Plk1 alone had little effect on cell viability. The reduced number of viable cells caused by exogenous p53 was recovered by co-expression of FLAG-Plk1. Considering that p53 induced apoptosis in transfected H1299 cells (47), Plk1 might abrogate the pro-apoptotic function of p53. To confirm this possibility, H1299 cells were transiently co-transfected with a constant amount of the GFP expression plasmid together with the indicated combinations of the expression plasmids. Forty-eight hours after transfection, transfected cells were scored by fluorescence microscopy for the appearance of green fluorescence,

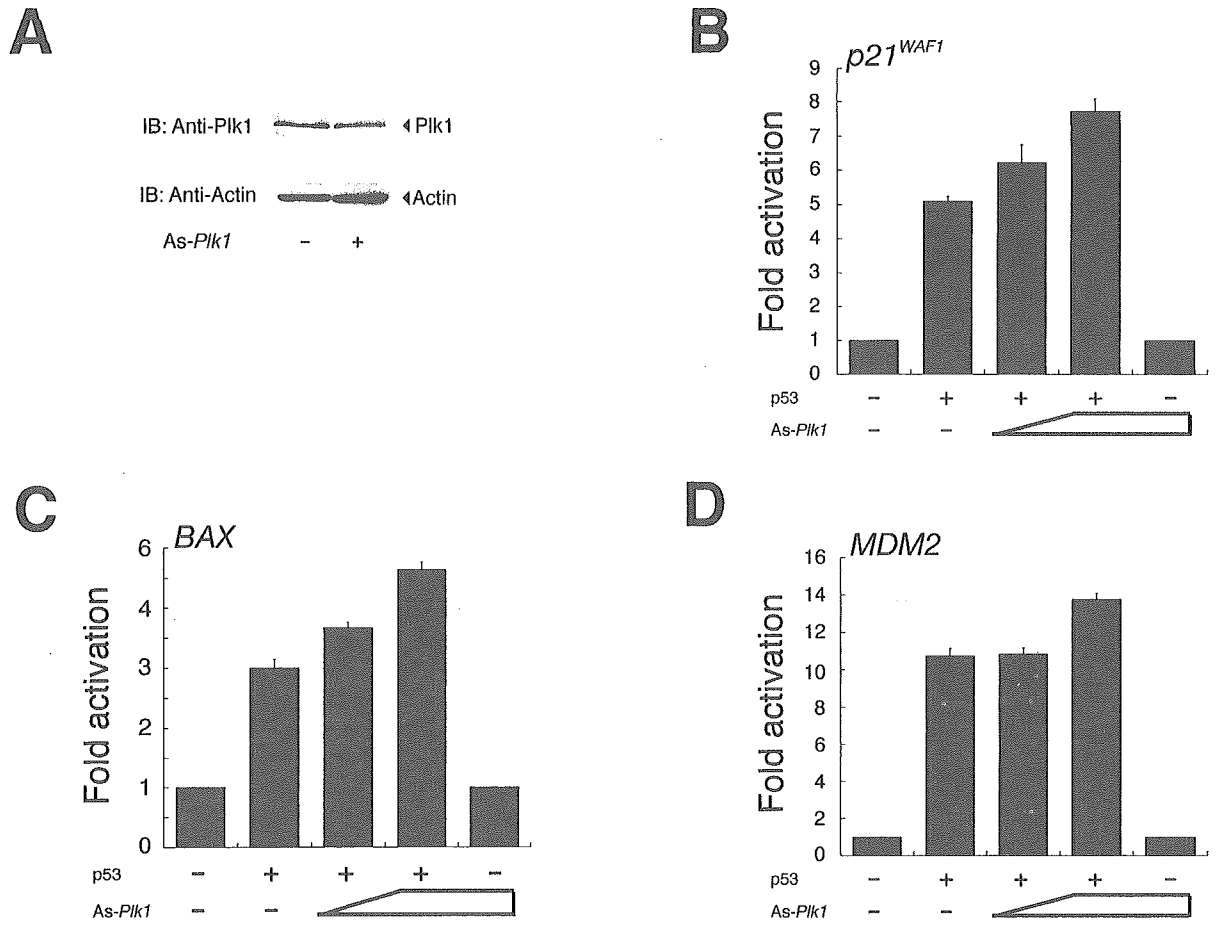

FIG. 7. **Antisense *Plk1* increases the transcriptional activity of p53.** *A*, antisense *Plk1* expression in H1299 cells results in a reduction of endogenous Plk1. H1299 cells were transfected with 2 μg of antisense *Plk1* expression plasmid (*As-Plk1*). Whole cell lysates prepared from transfected cells were subjected to immunoblotting with the anti-Plk1 antibody (*top panel*). Western blotting for actin is shown as a control for protein loading (*bottom panel*). *B–D*, luciferase reporter analysis. H1299 cells were transiently co-transfected with 12.5 ng of the p53 expression plasmid along with 100 ng of the indicated luciferase reporter construct in the presence or absence of increasing amounts of As-*Plk1* (200 and 400 ng). Determination and calculation of the luciferase activities are described in the legend to Fig. 6.

and the number of GFP-positive cells with condensed and fragmented nuclei were counted. Under our experimental conditions, enforced expression of p53 led to an increase in the number of apoptotic cells as compared with the control transfection (Fig. 8*B*). In agreement with the above cell survival assay, co-expression of p53 with FLAG-Plk1 decreased the number of apoptotic cells as compared with that resulting from expression of p53 alone. Taken together, these results indicate that Plk1 is an efficient inhibitor of p53.

Kinase-deficient Plk1 Fails to Inhibit p53—Next, we tested whether the Plk1 kinase activity could be required for Plk1-dependent inhibition of the p53 transcriptional activity. As described previously (22), the mutant form of Plk1 (Plk1-K82M), in which Lys^{82} within the ATP-binding motif is replaced by Met, completely lost the kinase activity. We therefore generated an expression plasmid encoding FLAG-Plk1(K82M), and then examined whether Plk1(K82M) could associate with p53, and also affect the p53-mediated transcriptional activation. Immunoprecipitation followed by Western detection of endogenous p53 indicated that p53 interacted with both the wild-type Plk1 and the kinase-deficient Plk1(K82M) (Fig. 9*A*). The effects of the lysine mutation on the p53-mediated transcriptional activation were tested by luciferase reporter analysis. In contrast to the wild-type Plk1, the kinase-deficient Plk1(K82M) failed to reduce the p53-mediated reporter expression driven by those constructs (Fig. 9, *B–D*).

To examine the effect of Plk1(K82M) on p53-dependent apoptosis, H1299 cells were transfected with the expression plasmid for p53 along with or without the expression plasmid for FLAG-Plk1(K82M). Forty-eight hours after transfection, their viability was measured by cell survival assay. As expected, the p53-dependent decrease in the number of viable cells was unaffected in the presence of the exogenous FLAG-Plk1(K82M) (Fig. 9*E*). Taken together, our results strongly suggest that the kinase activity of Plk1 is required for Plk1-dependent inhibition of p53.

ATM Antagonizes the Inhibitory Effect of Plk1 on p53—Plk1 kinase activity has been shown to be inhibited in an ATM-dependent manner in response to DNA damage (19, 20). The kinase activity of ATM was significantly increased after DNA damage, and ATM was able to phosphorylate p53 at the NH_2 terminus on serine 15 to enhance its stability as well as its transactivation activity (48–50). To examine whether ATM could affect the Plk1-mediated inhibition of p53, we transiently co-transfected H1299 cells with expression plasmids for p53 and FLAG-Plk1 together with or without increasing amounts of ATM expression plasmid, and the ability of p53 to drive transcription from the *p21^{WAF1}* reporter was measured. As expected, co-expression of p53 with ATM resulted in an increase in the transcriptional activity of p53 as compared with that of cells expressing p53 alone (Fig. 10). Increasing amounts of ATM largely abrogated the Plk1-mediated inhibition of the p53-dependent transcriptional activation. It thus appears that ATM could inhibit the activity of Plk1 and thereby restore the transcriptional activity of p53.

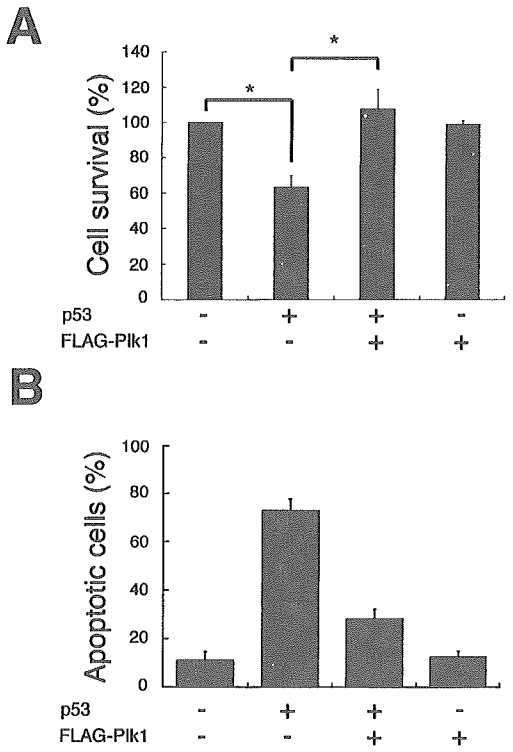

FIG. 8. **Plk1 inhibits the pro-apoptotic activity of p53.** *A*, H1299 cells were transiently co-transfected with 0.6 μg of the expression plasmid for p53 together with or without 1.2 μg of the FLAG-Plk1 expression plasmid. The total amount of plasmid DNA was kept constant (2 μg) with the empty plasmid. At 48 h after transfection, cell viability was determined by MTT cell survival assays. The graph (mean ± S.D. of three independent experiments) represents relative viability based on the percent of viable cells compared with the control transfection (pcDNA3). The percentage of viable cells expressing p53 alone is significantly different from that of viable cells expressing p53 and FLAG-Plk1 ($p < 0.0001$). *B*, H1299 cells were transiently co-transfected with the indicated combinations of the expression plasmids. A constant amount of the GFP expression plasmid (200 ng) was included in all combinations, and the total amount of plasmid DNA was kept constant (2 μg) by including an appropriate amount of empty plasmid. Forty-eight hours after transfection, transfected cells were identified by the presence of green fluorescence. Cell nucleus was stained with propidium iodide to reveal nuclear condensation and fragmentation. The number of GFP-positive cells with condensed and fragmented nuclei was scored, and the percentage of apoptotic cells shown in each column represents the mean of three independent experiments.

DISCUSSION

In the present study, we have found that Plk1 interacts with p53 and inhibits its transactivation as well as apoptosis-inducing activity in mammalian cultured cells. This interaction is mediated by the sequence-specific DNA-binding domain of p53 and the region of Plk1 containing the kinase domain. Importantly, Plk1-mediated inhibition of p53 requires its kinase activity and is attenuated with ATM. Thus, our present data support the hypothesis that p53 is one of the critical targets of Plk1, and that Plk1-mediated inhibition of p53 contributes at least in part to cell fate decisions regarding survival and tumorigenesis.

The expression of *Plk1* was significantly down-regulated in response to cisplatin treatment. Recently, Ree *et al.* (51) found that ionizing radiation leads to the suppression of *Plk1* mRNA expression. It is of interest to examine whether genotoxic stresses other than cisplatin and ionizing radiation could also repress the expression of *Plk1*. On the other hand, *Plk1* mRNA expression is significantly induced in various human primary tumors (27). It is necessary to identify the promoter region as well as the transcription factor(s) required for the transcriptional regulation of *Plk1* in cancerous cells. In good agreement with the previous observations (52), Uchiumi *et al.* (53) have identified the regulatory regions responsible for the activation of the human *Plk1* promoter, which include a consensus Sp1-binding site and a CCAAT box. It has been shown that the transcription factor NF-Y, a heterotrimeric complex consisting of NF-YA, NF-YB, and NF-YC, recognizes and binds to the CCAAT box (54). Indeed, the electrophoretic mobility shift assay revealed that NF-Y binds to the CCAAT box present within the human *Plk1* promoter region, however, it remains to be determined whether NF-Y and/or Sp1 could actually transactivate the *Plk1* promoter in tumor cells (53). Recently, Lee and Pedersen (55) have reported that there exist 6 GC boxes and the CCAAT box within the *type II hexokinase* (*HKII*) promoter, and that NF-Y and Sp family members including Sp1 might contribute to up-regulation of the *HKII* gene in tumor cells. Further studies regarding the transcriptional regulation of the *Plk1* gene are necessary to clarify the molecular mechanisms of Plk1-dependent tumorigenesis.

During the DNA damage response, the activity of ATM is significantly increased and is responsible for the rapid phosphorylation of p53 at Ser^{15} (48–50). This ATM-dependent phosphorylation contributes to the increased stability and activity of p53 by facilitating its dissociation from MDM2 (56). In addition, phosphorylation of p53 at Ser^{15} induces its binding to the transcriptional co-activator p300 (57). Recently, it has been shown that Plk1 activity is inhibited in response to DNA damage, and this inhibition occurs in an ATM-dependent manner (19, 20). Our present data demonstrate that the Plk1-mediated inhibition of p53 activity is rescued by the co-expression of ATM, suggesting that, in addition to the ATM-dependent phosphorylation of p53, the activity of p53 may be enhanced at least in part by the ATM-dependent inhibition of Plk1. Intriguingly, Liu and Erikson (33) reported that p53 is significantly stabilized in Plk1-depleted cells. In accordance with their findings, we have shown that the exposure of SH-SY5Y cells to cisplatin leads to a remarkable accumulation of p53, which is strongly associated with a significant down-regulation of the endogenous Plk1 both at mRNA and protein levels, suggesting that Plk1 is closely involved in the regulation of p53 stability and thereby modulates its activity. Under our experimental conditions, however, overexpression of FLAG-Plk1 did not affect the amounts of the endogenous as well as the ectopically expressed p53.

The pro-apoptotic function of p53 involves its ability to act as a transcription factor in transactivating downstream target gene promoters. The majority of missense mutations of p53 detected in human tumors occur within its sequence-specific DNA-binding domain, and these mutations cause the loss of p53 activity (58). Thus, the structural integrity of this domain is required for p53 function. On the other hand, several viral and cellular proteins inactivate p53 through a variety of different mechanisms (58). MDM2 and Pirh2 promote ubiquitination and degradation of p53 (59–62). Sir2α interacts with p53 and induces its deacetylation (63). In addition, S100B calcium-binding protein prevents the oligomerization of p53 to inhibit its function (64). Based on our systematic immunoprecipitation analysis, Plk1 binds to p53 through the sequence-specific DNA-binding domain of p53. Intriguingly, SV40 large T antigen binds to the sequence-specific DNA-binding domain of p53, and abrogates DNA binding as well as the transactivation function of p53 (65, 66). It is thus likely that, like SV40 large T antigen, Plk1 might mask this domain of p53 by direct binding, and thereby inhibit its sequence-specific transcriptional activity. Further study is required to identify the detailed molecular mechanism.

In sharp contrast to Plk1, Xie *et al.* (26) found that the kinase

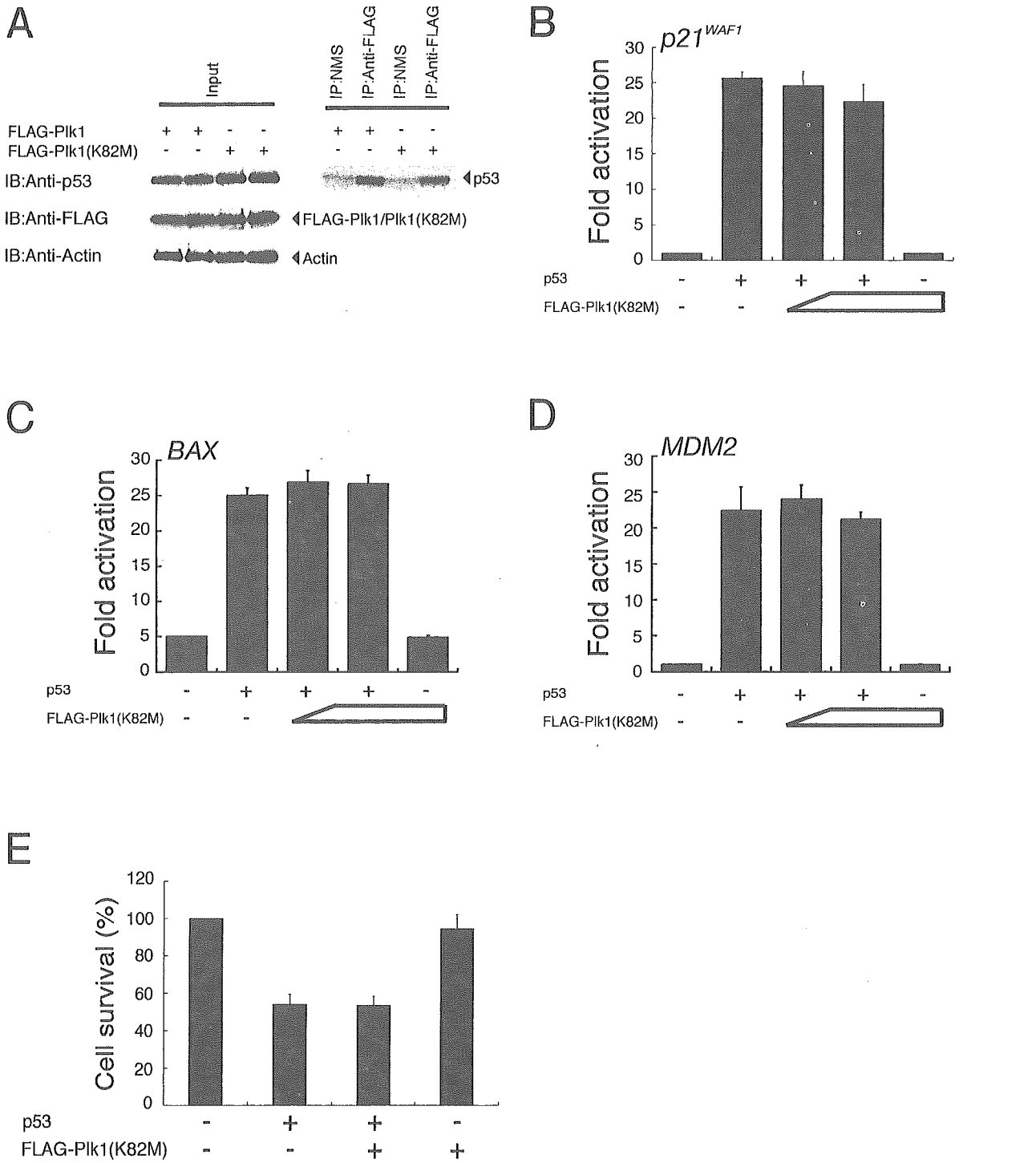

FIG. 9. **Kinase-deficient Plk1(K82M) fails to reduce the activity of p53.** *A*, Plk1(K82M) retains an ability to interact with p53. COS7 cells were transiently transfected with the expression plasmid for FLAG-Plk1 or FLAG-Plk1(K82M). Forty-eight hours after transfection, cell lysates were prepared and subjected to anti-FLAG immunoprecipitation followed by immunoblotting with monoclonal anti-p53 antibody. Immunoprecipitation with NMS was used as a negative control. Equal amounts of protein derived from cell lysates were immunoblotted with monoclonal anti-p53, monoclonal anti-FLAG, or with polyclonal anti-actin antibody. *B–D*, Plk1(K82M) has an undetectable effect on the transcriptional activity of p53. H1299 cells were transiently co-transfected with a fixed amount of the p53 expression plasmid (25 ng) and the p53-responsive luciferase reporter construct carrying the $p21^{WAF1}$ (*B*), *BAX* (*C*), or *MDM2* (*D*) promoter (100 ng) in the presence or absence of increasing amounts of the expression plasmid encoding FLAG-Plk1(K82M) (100 or 200 ng). The total amount of plasmid DNA per transfection was kept constant (510 ng) with pcDNA3. Determination and calculation of the luciferase activities are described in the legend to Fig. 6. *E*, Plk1(K82M) is unable to inhibit the pro-apoptotic function of p53. H1299 cells were transiently co-transfected with the p53 expression plasmid (0.6 μg) together with or without the expression plasmid for FLAG-Plk1(K82M) (1.2 μg). Forty-eight hours after transfection, their viability was measured by MTT cell survival assays as described in the legend to Fig. 8.

activity of Plk3 is rapidly enhanced in response to DNA damage in an ATM-dependent fashion. They also described that Plk3 has the ability to interact directly with p53 and phosphorylate p53 at Ser^{20}. Moreover, a kinase-defective mutant form of Plk3 fails to phosphorylate p53, and abrogates the p53-mediated transcriptional activation as well as growth suppression, indicating that Plk3 might enhance the p53 activity through Ser^{20} phosphorylation of p53 (26). In addition to Ser^{15} phosphoryla-

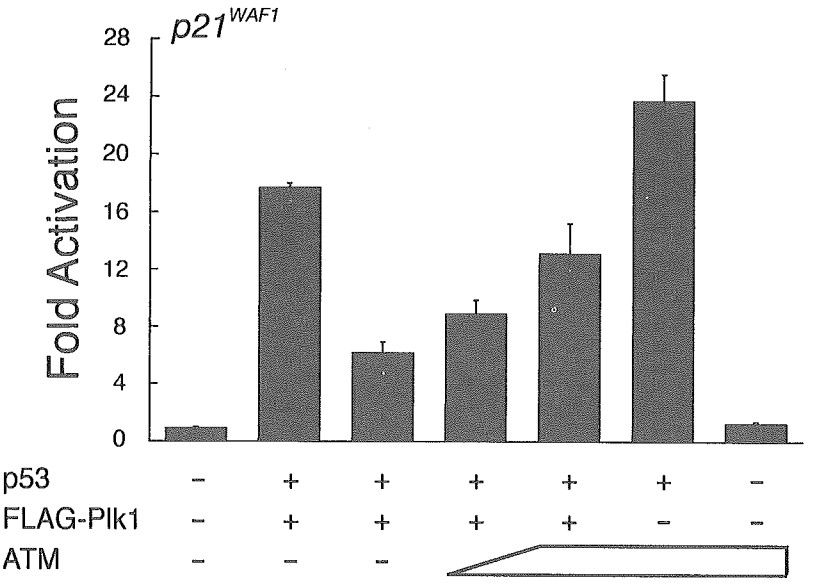

FIG. 10. **ATM antagonizes the inhibitory effect of Plk1 on the p53-dependent transactivation.** H1299 cells were transiently co-transfected with the expression plasmids encoding p53 (25 ng) and FLAG-Plk1 (200 ng) along with the luciferase reporter construct containing the p53-responsive element from the $p21^{WAF1}$ promoter in the presence or absence of increasing amounts of ATM expression plasmid (50 or 100 ng). pcDNA3 was used to equalize the amount of plasmid in each transfection, and the *Renilla* luciferase plasmid was included in the transfection mixture to normalize the transfection efficiency. Determination and calculation of the luciferase activities are described in the legend to Fig. 6.

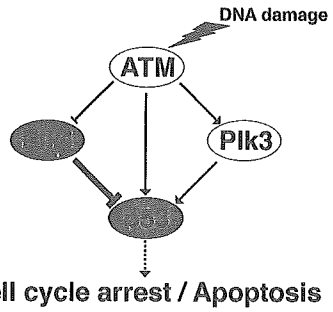

FIG. 11. **Schematic representation of interactions among ATM, Plk1, Plk3, and p53 in response to DNA damage.**

tion of p53, DNA damage-induced phosphorylation of p53 at Ser^{20} prevents its association with MDM2 and results in its stabilization (67). Of note, it has been shown that Plk1 phosphorylates p53 *in vitro* but on residues that might be different from that mediated by Plk3 (26). According to their phosphopeptide mapping analysis, at least three unique radiolabeled tryptic peptides derived from recombinant p53 were detected in the presence of Plk1. Recently, Nakajima *et al.* (68) identified a sequence (D/E)*X*(S/T)ψ*X*(D/E) (*X*, any amino acid; ψ, a hydrophobic amino acid) as a consensus motif for Plk1-dependent phosphorylation (68). During the search for a putative phosphorylation site(s) targeted by Plk1 within the amino acid sequence of p53, we found a related motif (^{254}IITLED^{259}) present within the sequence-specific DNA-binding domain of p53, suggesting that this motif could be one of the putative phosphorylation sites of p53 targeted by Plk1, although there is no direct evidence for this possibility. According to our present results, the kinase-deficient mutant form of Plk1 that retained an ability to associate with p53, failed to reduce the transcriptional as well as apoptosis-inducing activity of p53, suggesting that the kinase activity of Plk1 is critical for the Plk1-dependent inhibition of p53. Thus, identification of the major phosphorylation site(s) of p53 by Plk1 is required to establish the functional significance of the Plk1-mediated phosphorylation of p53. In contrast, Liu and Erikson (33) reported that, like wild-type mouse Plk1, co-expression of the kinase-defective (K82M) mouse Plk1 partially rescued the apoptotic phenotype induced by the depletion of Plk1, indicating that the kinase activity is not necessary for its anti-apoptotic activity. They also described that their kinase-defective mouse Plk1 has 15–20% of wild-type kinase activity, raising a possibility that the residual kinase activity of their mouse Plk1(K82M) might be enough to inhibit the Plk1 depletion-induced apoptosis.

Fig. 11 shows a model that incorporates our present findings, and illustrates various interactions in response to DNA damage. Given the fact that the differential expression of Plk1 and Plk3 during the cisplatin-induced apoptosis, and their differential effects on p53, it is conceivable that the balance between intracellular expression levels of Plk1 with oncogenic potential and pro-apoptotic Plk3 is at least in part responsible for the determination of the cell fate via the physical and functional interaction with p53.

Acknowledgments—We are grateful to Dr. Y. Shiloh and the Japanese Study Group for Pediatric Liver Tumor for kindly providing the ATM expression plasmid and hepatoblastoma tissues, respectively. We thank Dr. S. Sakiyama and members of our laboratory for helpful discussions. We also thank Y. Nakamura and M. Kikawa for excellent technical assistance.

REFERENCES

1. Glover, D. M., Hagan, I. M., and Tavares, A. A. (1998) *Genes Dev.* **12,** 3777–3787
2. Clay, F. J., McEwen, S. J., Bertoncello, I., Wilks, A. F., and Dunn, A. R. (1993) *Proc. Natl. Acad. Sci. U. S. A.* **90,** 4882–4886
3. Lee, K. S., Grenfell, T. Z., Yarm, F. R., and Erikson, R. L. (1998) *Proc. Natl. Acad. Sci. U. S. A.* **95,** 9301–9306
4. Song, S., Grenfell, T., Garfield, S., Erikson, R. L., and Lee, K. S. (2000) *Mol. Cell. Biol.* **20,** 286–298
5. Jang, Y.-J., Lin, C.-Y., Ma, S., and Erikson, R. L. (2002) *Proc. Natl. Acad. Sci. U. S. A.* **99,** 1984–1989
6. Glover, D. M., Ohkura, H., and Tavares, A. (1996) *J. Cell Biol.* **135,** 1681–1684
7. Lane, H., and Nigg, E. A. (1997) *Trends Cell. Biol.* **7,** 63–68
8. Nigg, E. A. (1998) *Curr. Opin. Cell Biol.* **10,** 776–783
9. Hamanaka, R., Maloid, S., Smith, M. R., O'Connell, C. D., Longo, D. L., and Ferris, D. K. (1994) *Cell Growth & Differ.* **5,** 249–257
10. Smith, M. R., Wilson, M. L., Hamanaka, R., Chase, D., Kung, H.-F., Longo, D. L., and Ferris, D. K. (1997) *Biochem. Biophys. Res. Commun.* **234,** 397–405
11. Lake, R. J., and Jelinek, W. R. (1993) *Mol. Cell. Biol.* **13,** 7793–7801
12. Golsteyn, R. M., Schultz, S. J., Bartek, J., Ziemiecki, A., Ried, T., and Nigg, E. A. (1994) *J. Cell Sci.* **107,** 1509–1517
13. Holtrich, U., Wolf, G., Brauninger, A., Karn, T., Bohme, B., Rubsamen-Waigmann, H., and Strebhardt, K. (1994) *Proc. Natl. Acad. Sci. U. S. A.* **91,** 1736–1740
14. Simmons, D. L., Neel, B. G., Stevens, R., Evett, G., and Erikson, R. L. (1992) *Mol. Cell. Biol.* **12,** 4164–4169
15. Donohue, P. J., Alberts, G. F., Guo, Y., and Winkles, J. A. (1995) *J. Biol. Chem.* **270,** 10351–10357
16. Golsteyn, R. M., Mundt, K. E., Fry, A. M., and Nigg, E. A. (1995) *J. Cell Biol.* **129,** 1617–1628
17. Hamanaka, R., Smith, M. R., O'Connor, P. M., Maloid, S., Mihalic, K., Spivak, J. L., Longo, D. L., and Ferris, D. K. (1995) *J. Biol. Chem.* **270,** 21086–21091
18. Qian, Y.-W., Erikson, E., and Maller, J. L. (1998) *Science* **282,** 1701–1704
19. Smits, V. A., Klompmaker, R., Arnaud, L., Rijksen, G., Nigg, E. A., and Medema, R. H. (2000) *Nat. Cell Biol.* **2,** 672–676
20. van Vugt, M. A. T. M., Smits, V. A. J., Klompmaker, R., and Medema, R. H. (2001) *J. Biol. Chem.* **276,** 41656–41660
21. Toyoshima-Morimoto, F., Taniguchi, E., Shinya, N., Iwamatsu, A., and

Nishida, E. (2001) *Nature* **410,** 215–220
22. Yuan, J., Eckerdt, F., Bereiter-Hahn, J., Kurunci-Csacsko, E., Kaufmann, M., and Strebhardt, K. (2002) *Oncogene* **21,** 8282–8292
23. Toyoshima-Morimoto, F., Taniguchi, E., and Nishida, E. (2002) *EMBO Rep.* **3,** 341–348
24. Ouyang, B., Pan, H., Lu, L., Li, J., Stambrook, P., Li, B., and Dai, W. (1997) *J. Biol. Chem.* **272,** 28646–28651
25. Bahassi, E. M., Conn, C. W., Myer, D. L., Hennigan, R. F., McGowan, C. H., Sanchez, Y., and Stambrook, P. J. (2002) *Oncogene* **21,** 6633–6640
26. Xie, S., Wu, H., Wang, Q., Cogswell, J. P., Husain, I., Conn, C., Stambrook, P., Jhanwar-Uniyal, M., and Dai, W. (2001) *J. Biol. Chem.* **276,** 43305–43312
27. Yuan, J., Horlin, A., Hock, B., Stutte, H. J., Rubsamen-Waigmann, H., and Strebhardt, K. (1997) *Am. J. Pathol.* **150,** 1165–1172
28. Wolf, G., Elez, R., Doermer, A., Holtrich, U., Ackermann, H., Stutte, H. J., Altmannsberger, H. M., Rubsamen-Waigmann, H., and Strebhardt, K. (1997) *Oncogene* **14,** 543–549
29. Knecht, R., Elez, R., Oechler, M., Solbach, C., von Ilberg, C., and Strebhardt, K. (1999) *Cancer Res.* **59,** 2794–2797
30. Knecht, R., Oberhauser, C., and Strebhardt, K. (2000) *Int. J. Cancer* **89,** 535–536
31. Spankuch-Schmitt, B., Wolf, G., Solbach, C., Loibl, S., Knecht, R., Stegmuller, M., von Minckwitz, G., Kaufmann, M., and Strebhardt, K. (2002) *Oncogene* **21,** 3162–3171
32. Spankuch-Schmitt, B., Bereiter-Hahn, J., Kaufmann, M., and Strebhardt, K. (2002) *J. Natl. Cancer Inst.* **94,** 1863–1877
33. Liu, X., and Erikson, R. L. (2003) *Proc. Natl. Acad. Sci. U. S. A.* **100,** 5789–5794
34. Li, B., Ouyang, B., Pan, H., Reissmann, P. T., Slamon, D. J., Arceci, R., Lu, L., and Dai, W. (1996) *J. Biol. Chem.* **271,** 19402–19408
35. Dai, W., Li, Y., Ouyang, B., Pan, H., Reissmann, P., Li, J., Wiest, J., Stambrook, P., Gluckman, J. L., Noffsinger, A., and Bejarano, P. (2000) *Genes Chromosomes Cancer* **27,** 332–336
36. Conn, C. W., Hennigan, R. F., Dai, W., Sanchez, Y., and Stambrook, P. J. (2000) *Cancer Res.* **60,** 6826–6831
37. Xie, S., Wang, Q., Wu, H., Cogswell, J., Lu, L., Jhanwar-Uniyal, M., and Dai, W. (2001) *J. Biol. Chem.* **276,** 36194–36199
38. Nakamura, Y., Ozaki, T., Nakagawara, A., and Sakiyama, S. (1997) *Eur. J. Cancer* **33,** 1986–1990
39. Nakagawa, T., Takahashi, M., Ozaki, T., Watanabe, K., Todo, S., Mizuguchi, H., Hayakawa, T., and Nakagawara, A. (2002) *Mol. Cell. Biol.* **22,** 2575–2585
40. Watanabe, K., Ozaki, T., Nakagawa, T., Miyazaki, K., Takahashi, M., Hosoda, M., Hayashi, S., Todo, S., and Nakagawara, A. (2002) *J. Biol. Chem.* **277,** 15113–15123
41. Kim, E.-J., Park, J.-S., and Um, S.-J. (2002) *J. Biol. Chem.* **277,** 32020–32028
42. Taniguchi, E., Totoshima-Morimoto, F., and Nishida, E. (2002) *J. Biol. Chem.* **277,** 48884–48888
43. Kastan, M. B., Zhan, Q., el-Deiry, W. S., Carrier, F., Jacks, T., Walsh, W. V., Plunkett, B. S., Vogelstein, B., and Fornace, A. J., Jr. (1992) *Cell* **71,** 587–597
44. Shaulsky, G., Goldfinger, N., Ben-Ze'ev, A., and Rotter, V. (1990) *Mol. Cell. Biol.* **10,** 6565–6577
45. Dang, C. V., and Lee, W. M. (1989) *J. Biol. Chem.* **264,** 18019–18023
46. Zaika, A. I., Slade, N., Erster, S. H., Sansome, C., Joseph, T. W., Pearl, M., Chalas, E., and Moll, U. M. (2002) *J. Exp. Med.* **196,** 765–780
47. Zeng, X., Chen, L., Jost, C. A., Maya, R., Keller, D., Wang, X., Kaelin, W. G., Oren, M., Chen, J., and Lu, H. (1999) *Mol. Cell. Biol.* **19,** 3257–3266
48. Banin, S., Moyal, L., Shieh, S., Taya, Y., Anderson, C. W., Chessa, L., Smorodinsky, N. I., Prives, C., Reiss, Y., Shiloh, Y., and Ziv, Y. (1998) *Science* **281,** 1674–1677
49. Canman, C. E., Lim, D. S., Cimprich, K. A., Taya, Y., Tamai, K., Sakaguchi, K., Appella, E., Kastan, M. B., and Siliciano, J. D. (1998) *Science* **281,** 1677–1679
50. Khanna, K. K., Keating, K. E., Kozlov, S., Scott, S., Gatei, M., Hobson, K., Taya, Y., Gabrielli, B., Chan, D., Lees Miller, S. P., and Lavin, M. F. (1998) *Nat. Genet.* **20,** 398–400
51. Ree, A. H., Bratland, A., Nome, R. V., Stokke, T., and Fodstad, O. (2003) *Oncogene* **22,** 8952–8955
52. Brauninger, A., Strebhardt, K., and Rubsamen-Waigmann, H. (1995) *Oncogene* **11,** 1793–1800
53. Uchiumi, T., Longo, D. L., and Ferris, D. K. (1997) *J. Biol. Chem.* **272,** 9166–9174
54. Mantovani, R. (1999) *Gene (Amst.)* **239,** 15–27
55. Lee, M. G., and Pedersen, P. L. (2003) *J. Biol. Chem.* **278,** 41047–41058
56. Shieh, S. Y., Ikeda, M., Taya, Y., and Prives, C. (1997) *Cell* **91,** 325–334
57. Lambert, P. F., Kashanchi, F., Radonovich, M. F., Shiekhattar, R., and Brady, J. N. (1998) *J. Biol. Chem.* **273,** 33048–33053
58. Prives, C., and Hall, P. A. (1999) *J. Pathol.* **187,** 112–126
59. Haupt, Y., Maya, R., Kazaz, A., and Oren, M. (1997) *Nature* **387,** 296–299
60. Kubbutat, M. H. G., Jones, S. N., and Vousden, K. H. (1997) *Nature* **387,** 299–303
61. Honda, R., Tanaka, H., and Yasuda, Y. (1997) *FEBS Lett.* **420,** 25–27
62. Leng, R. P., Lin, Y., Ma, W., Wu, H., Lemmers, B., Chung, S., Parant, J. M., Lozano, G., Hakem, R., and Benchimol, S. (2003) *Cell* **112,** 779–791
63. Luo, J., Nikolaev, A. Y., Imai, S., Chen, D., Su, F., Shiloh, A., Guarente, L., and Gu, W. (2001) *Cell* **107,** 137–148
64. Lin, J., Blake, M., Tang, C., Zimmer, D., Rustandi, R. R., Weber, D. J., and Carrier, F. (2001) *J. Biol. Chem.* **276,** 35037–35041
65. Tan, T.-H., Wallis, J., and Levine, A. J. (1986) *J. Virol.* **59,** 574–583
66. Farmer, G., Bargonetti, J., Zhu, H., Friedman, P., Prywes, R., and Prives, C. (1992) *Nature* **358,** 83–86
67. Vousden, K. H. (2002) *Biochim. Biophys. Acta* **1602,** 47–59
68. Nakajima, H., Toyoshima-Morimoto, F., Taniguchi, E., and Nishida, E. (2003) *J. Biol. Chem.* **278,** 25277–25280